Personalizing treatment for malignant pleural mesothelioma

Quispel-Janssen, J.M.M.F.

CHAPTER 5

5

Comprehensive Pharmacogenomic Profiling of Malignant Pleural Mesothelioma Identifies a Subgroup Sensitive to FGFR Inhibition

Josine M. Quispel-Janssen[1] | Jitendra Badhai[1] | Laurel Schunselaar[1] | Stacey Price[2] | Jonathan Brammeld[2] | Francesco Iorio[3] | Krishna Kolluri[4] | Matthew Garnett[2] | Anton Berns[1], Paul Baas[1] | Ultan McDermott[2] | Jacques Neefjes[1] | Constantine Alifrangis[2]

Clinical Cancer Research; 24(1); 84–94 2017

Abstract

Purpose: Despite intense research, treatment options for patients with mesothelioma are limited and offer only modest survival advantage. We screened a large panel of compounds in multiple mesothelioma models and correlated sensitivity with a range of molecular features to detect biomarkers of drug response.

Experimental design: We utilized a high-throughput chemical inhibitor screen in a panel of 889 cancer cell lines, including both immortalized and primary early-passage mesothelioma lines, alongside comprehensive molecular characterization using Illumina whole-exome sequencing, copy-number analysis and Affymetrix array whole transcriptome profiling. Subsequent validation was done using functional assays such as siRNA silencing and mesothelioma mouse xenograft models.

Results: A subgroup of immortalized and primary MPM lines appeared highly sensitive to FGFR inhibition. None of these lines harbored genomic alterations of FGFR family members, but rather BAP1 protein loss was associated with enhanced sensitivity to FGFR inhibition. This was confirmed in an MPM mouse xenograft model and by BAP1 knockdown and overexpression in cell line models. Gene expression analyses revealed an association between BAP1 loss and increased expression of the receptors FGFR1/3 and ligands FGF9/18. BAP1 loss was associated with activation of MAPK signaling. These associations were confirmed in a cohort of MPM patient samples.

Conclusions: A subgroup of mesotheliomas cell lines harbor sensitivity to FGFR inhibition. BAP1 protein loss enriches for this subgroup and could serve as a potential biomarker to select patients for FGFR inhibitor treatment. These data identify a clinically relevant MPM subgroup for consideration of FGFR therapeutics in future clinical studies.

Translational Relevance

Malignant pleural mesothelioma (MPM) has limited treatment options and a dismal prognosis. To date, targeted therapies have proved ineffective, and no druggable genetic alterations have been identified. Selecting compounds for further clinical evaluation in this small and heterogeneous patient group is challenging. By combining high-throughput drug screens, comprehensive molecular characterization and functional assays in multiple mesothelioma models, we were able to identify an FGFR inhibitor-sensitive subgroup with BAP1 loss as a potential predictive biomarker. Loss of BAP1 is found in up to 64% of MPM tumors. These data suggest that a significant group of patients with mesothelioma may benefit from FGFR inhibition.

Introduction

Malignant pleural mesothelioma (MPM) is a tumor arising from the pleural cavity and is strongly associated with occupational exposure to asbestos. Although strict regulation is in place in more than 50 countries, in parts of the world where there is still widespread usage of asbestos, most notably in South America, Russia, and states of the former Soviet Republic, China, and South-East Asia, the incidence of this disease is rising (1, 2). MPM is highly refractory to conventional anticancer therapies, and the prognosis is poor; most patients die within a year of diagnosis. Surgery with curative intent is only possible in a highly selected group of patients and needs to be combined with chemotherapy. The only approved treatment, a combination of the cytotoxic agents cisplatin and pemetrexed, yields at best modest improvements in survival (3, 4). Despite many clinical studies utilizing novel biological therapies, there are as yet no effective targeted therapies for this cancer (5, 6).

A recent comprehensive genomic analysis of 216 MPM samples found BAP1, NF2, TP53, SETD2, and CDKN2A to be recurrently mutated or structurally rearranged (7). The landscape is thus one of mutated tumor suppressor genes and alterations in pathways as diverse as Hippo, mTOR, and TP53, as well as histone methylation. Such loss-of-function oncogenic events are typically considered "undruggable," but downstream programs of genes, activated as a consequence of such mutations, may themselves be tractable therapeutic targets. This is illustrated by NF2-deficient tumors with activated focal adhesion kinase (FAK). Defactinib, a FAK inhibitor, demonstrated efficacy in NF2-deficient tumors in vitro (8) but a subsequent clinical trial in mesothelioma was halted due to lack of efficacy. Other drugs tested to date that have failed to improve the outcome in MPM include EGFR inhibitors (9), Bcr–Abl inhibitors (10), thalidomide (11), bortezomib (12), and vorinostat (13). In many of these studies, a subgroup of patients appeared to derive some benefit. However, in MPM, it has been difficult to elucidate reproducible biomarkers that identify these sensitive subgroups. Some research groups have demonstrated coactivation of multiple RTK pathways in MPM tumors, which may provide a rationale for combination therapies with kinase inhibitors (14).

We aimed to utilize high-throughput chemical screening platforms alongside molecular characterization of immortalized and early-passage cell line models of MPM to uncover critical signaling pathways that may be amenable to therapeutic interrogation.

Materials and Methods

Cell lines and tissue culture

Cells are grown and maintained in either RPMI or DMEM F/12 supplemented with 10% FBS and 1% penicillin/streptomycin. Cell lines were maintained at 37^{o} C at 5% CO_2. All cell lines have been verified by genotyping using short tandem repeat (STRs) profiling and Sequenom profiling of a panel of 92 single-nucleotide polymorphisms.

Cell viability assays

Cells are trypsinized and counted before seeding at the optimal density for the well size (either 96-or 384-well plates were used) and duration of the assay. Seeding density was optimized by titration of the cells such that upon visual inspection of the control wells at the end of the assay, a confluency of 70% to 90% was observed allowing cells to grow in a linear phase. Adherent cell lines were seeded 24 hours before drug addition. The high-throughput chemical inhibitor screen was carried out using 384-well plates, and viability was measured 72 hours after drug addition with a 5-point serial fourfold concentration range of 265 compounds. All other viability assays were carried out using 96-well plates and a 9-point twofold dilution of the drugs. Drugs were all dissolved in DMSO, and DMSO was used only as a control condition. At the end of the experiment, cells were fixed with 4% paraformaldehyde. Following two washes with dH_2O, 100 mL of Syto60 nucleic acid stain (Invitrogen) was added to a final concentration of 1 mmol/L (a 1/5,000 stock dilution), and plates were fixed for 1 hour at room temperature. Quantification of fluorescent signal was achieved using a Paradigm (BD) plate reader using excitation/emission wavelengths of 630/695 nm. Data were analyzed by adjusting for background signals and normalizing each well to the DMSO-treated control.

High-throughput screening compounds

Compounds were acquired from academic collaborators or commercial vendors. Each compound, its therapeutically relevant target substrate and pathway, and the minimum and maximum screening concentrations are listed in Supplementary Table S1. Compounds were stored as 10 mmol/L aliquots at -80^{o} C and were subjected to a maximum of 5 freeze–thaw cycles. Each of the agents was screened at a 5-point serial fourfold dilution to provide a 256-fold range from the lowest to highest concentration. The concentrations selected for each compound were based on in vitro data to cover the range of concentrations known to inhibit relevant kinase activity and cell viability.

Apoptosis assay

Cells were seeded in a flat-bottom 384 wells plate at optimal cell density. After 24 hours, PD173074 and AZD 4547 in a concentration range between 0.007813 and 1 mmol/L were added using a Tecan HP D300 Digital Dispenser. Five replicate wells were assayed for each

condition. Phenylarsine oxide (20 mmol/L) was used as positive control condition. To assess apoptosis, 5 mmol/L of IncuCyte caspase-3/7 green apoptosis assay reagent was added to the cells. Confluence and apoptosis levels were quantified by IncuCyte Zoom live-cell imaging systems from Essen Bioscience. Relative apoptosis was calculated by dividing the confluence of fluorescent apoptotic cells by total confluence and normalized to the positive control condition.

Western blots

Cell monolayers were lysed on ice in NP40 Cell Lysis Buffer (Invitrogen) containing fresh protease and phosphatase inhibitors (Roche). Lysates were centrifuged at 13,000 rpm for 10 minutes and the supernatant used for analyses. Protein concentration was calculated from a standard curve of BSA using the BCA assay (calbiotech) according to the manufacturer's instructions. Equal protein concentrations were loaded on pre-cast 4% to 12% Bis-Tris SDS-PAGE Gels (Invitrogen), run at 200 V for 1 hour. Proteins were transferred onto a methanol activated PVDF membrane at 100 V for 1 hour or overnight at 30 V. Membranes were blocked in 5% milk for 1 hour before the addition of primary antibody at a concentration recommended. After overnight incubation with the primary antibody at 4^{O} C, the membrane was washed three times in 0.1% TBS-T followed by incubation with the secondary antibody according to the supplier's description at 1/2,500 dilution). Immunoblots were imaged using Pierce Supersignal Plus chemiluminescent kit on a gel imager (Syngene). Antibodies against BAP1, pERK, ERK, pFGFR (total), and pFGFR1 (all from Cell Signaling Technologies) and the polyclonal p-FGFR3 antibody sc-33041 (Santa Cruz Biotechnology) were used. Beta Tubulin was used as a loading control for Western blots. Phospho-RTK arrays (RD Systems) and caspase-Glo 3/7 assay were used according to the manufacturer's instructions.

Establishment of early-passage primary mesothelioma tumor cell cultures

All patients whose materials were used provided written informed consent for the use and storage of pleural fluid, tumor biopsies, and germline DNA. Diagnosis was made on tumor biopsies according to local IHC protocols and confirmed by the Dutch mesothelioma panel, a national expert panel of certified pathologists that evaluate all suspected mesothelioma patient samples. Early-passage primary mesothelioma cultures were generated from tumor cells isolated from pleural fluid of patients at the Netherlands Cancer Institute. The pleural fluid was centrifuged at 1,500 rpm for 5 minutes at room temperature. Erythrocyte lysis buffer was used to remove erythrocytes if many were present. Cells were resuspended in Dulbecco's Modified Eagle Medium (DMEM, Gibco) supplemented with peniciline/streptomycin and 8% fetal calf serum. The cells were seeded in T75 flasks at a density of 1 x 10^6 cells/mL and incubated at 37^{O} C at a humidified 5% CO_2 atmosphere. Medium was refreshed depending on cell growth, usually twice a week. At seeding and during the first two passages, cytospins were made and stained with HE and reviewed by our pathologist to determine the percentage of tumor cells. If the tumor percentage was over 70%, usually

reached after one passage, living cell cultures were transported to the Wellcome Trust Sanger Institute within 6 hours for drug screening and genetic analysis. Cells were cultured for a maximum period of 4 weeks.

RNA interference and transfection

Lipofectamine RNAiMAX (Thermofisher) was used according to product guidelines for transfection with siRNA against FGFR3 (Thermo Fisher Silencer Select s5167 and s5169) or BAP1 (s15822) utilizing the protocol "forward transfection of mammalian cell lines." KIF11 siRNA (s7902) was used as a transfection (positive) control. Viability or protein expression was assayed as described above, at specified time points. H226 cell expressing a BAP1 stable construct, and BAP1 C91A mutant lines were a kind gift from K Kolluri (UCL, London).

Gene expression analyses

Microarray data were generated on the Human Genome U219 96-Array Plate using the Gene Titan MC instrument (Affymetrix). The robust multi-array analysis (RMA) algorithm (15) was used to establish intensity values for each of 18562 loci (BrainArray v.10). We discarded transcripts with low sample variance and consolidated duplicated genes by averaging their expression values across duplicates. The resulting data were subsequently normalized (μ=0; σ= 1) sample-wise and gene-median centered. Raw data were deposited in ArrayExpress (accession E-MTAB-3610). The RMA processed dataset is available at www.cancerrxgene.org/gdsc1000/GDSC1000_WebResources/Home.html. The expression-level signal of each gene was normalized using a nonparametric kernel estimation of its cumulative density function as described in ref. 16. Additionally, the normalized expression values were further tissue-centered using as grouping factors the cell line tissue labels of ref. 17.

MPM mouse xenograft models

All animal experiments were conducted according to institutional guidelines under protocol approved by the animal ethics committee of the Netherlands Cancer Institute. To establish xenografts, 3 million human mesothelioma cells (H2731 and MSTO211H) were implanted subcutaneously into the right dorsal flank of 6- to 7-week-old female nude SCID mice. Mice were randomized into vehicle and drugs treatment groups, and treatment was initiated once the tumor volumes reached approximately 200 mm^3. Tumor size was measured with calipers twice a week, and tumor volume was determined as $a \times b^2 \times 0.5$, where a and b were the large and small diameters, respectively.

Results

High-throughput chemical inhibitor screens in immortalized cell lines

A panel of 889 cancer cell lines was screened with 265 compounds that included targeted and cytotoxic compounds (for detail see http://www.cancerrxgene.org/). It was observed that three of 19 MPM lines (H2795, H2591, and MSTO-211H) had IC_{50} values among the top 5% of cell lines showing highest sensitivity to the compound PD-173074, an FGFR1 and FGFR3 kinase inhibitor (Fig. 1A; ref. 15). These three cell lines, together with two additional MPM lines (NCI-H28, resistant; MPP-89, partially sensitive) and an FGFR-dependent lung cancer cell line harboring amplification of FGFR1 (NCI-H1581), were rescreened with PD-173074 and were as sensitive to PD-173074 as the FGFR1-dependent lung cancer line NCI-1581 (Fig. 1B). Furthermore, this sensitivity was also seen with two more selective FGFR inhibitors, NVP-BGJ398 and AZD4547 (Supplementary Fig. S1). Sensitivity to PD-173074 in the MPM cell lines was confirmed by clonogenic survival assays (Fig. 1C). Although some sensitive lines died by apoptosis, as is shown by activated caspase activity with both PD-173074 and the multi-FGFR-targeted inhibitor AZD4547 (Fig. 1D and E), not all sensitive lines showed a dose incremental increase in this marker. These data confirm previous findings (18) that a subset of MPM cell lines require FGF pathway activation for growth and survival, and that targeting this pathway could be a critical step in the control of these tumors.

Drug sensitivity in early-passage MPM cultures

To test whether these observations could be reproduced in an independent cohort of primary mesothelioma cell lines, a panel of 11 pleural fluid-derived early-passage cultures from patients with MPM tumors were obtained and screened for viability using a panel of 48 small molecule inhibitors including PD-173074. Most of the early-passage cultures were resistant to virtually all agents (Supplementary Fig. S2). However, one MPM early-passage culture (NKI04) did demonstrate marked sensitivity to PD-173074. The sensitivity of NKI04 to FGFR inhibition was confirmed in a longer duration clonogenic survival assay, and the effect on cell viability was comparable with that seen in the FGFR1-amplified NCI-H1581 lung cancer cell line (Fig. 2A-C).

Molecular characterization of FGF pathway signaling in cell lines and patient samples

In order to understand the basis for the observed sensitivity to FGFR inhibition, we analyzed whole-exome sequence and copy number array data for 21 MPM lines (http://cancer.sanger.ac.uk/cell_lines). There was no evidence of activating mutations or whole gene amplifications in any FGFR family member. RNA sequencing has been undertaken and shows no evidence of a fusion transcript involving any member of the FGFR family in any of the MPM cell lines (personal communication, M. Garnett). We then analyzed the corresponding gene expression data and focused on differential expression of FGFR and FGF family members in PD-173074-sensitive and -resistant MPM cell lines. Normalized expression of each of the FGF and FGFR

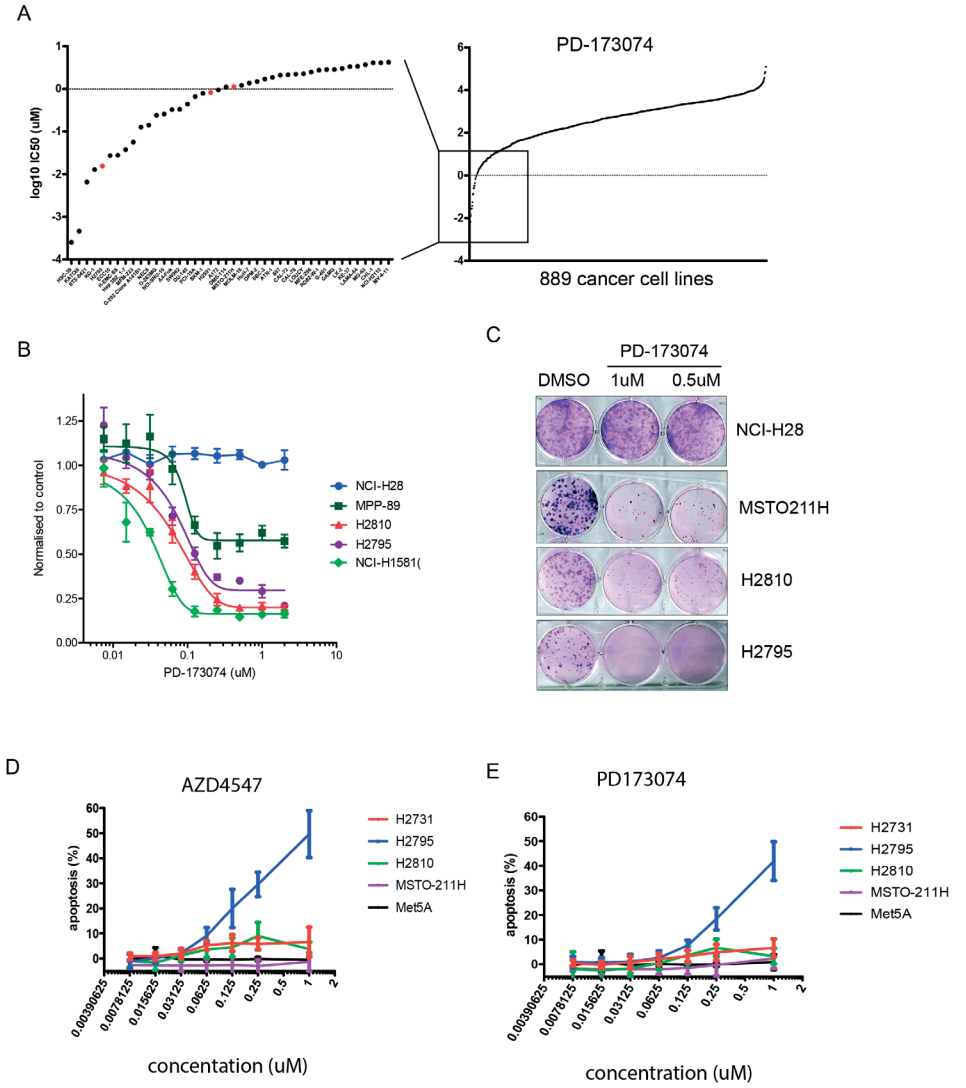

Figure 1. Sensitivity to FGFR inhibition in established mesothelioma cell lines.

(**A**) Sensitivity to FGFR inhibitor PD173074 expressed as logIC$_{50}$ value (inhibiting concentration that kills 50% of the cells) of each different cell line. The enlargement shows the 5% most sensitive cell lines with amongst them mesothelioma cell lines depicted in red. (**B**) Dose–response curves depicting the cell viability (mean ±SD) of different cell lines (y-axis) as a function of the dose of FGFR inhibitor PD-173074. NCI-H28, MPP-89, H2810, and H2795 are mesothelioma cell lines, while NCI-H1581 is an FGFR-dependent lung cancer cell line. (**C**) Fourteen-day clonogenic survival assay of selected mesothelioma cell lines (NCI-H28, MSTO-211H, H2810, and H2795), treated with FGFR inhibitor PD-173074 at concentrations of 500 nmol/L and 1 mmol/L. (**D**) FGFR inhibitor AZD4547 kills mesothelioma cell lines via induction of apoptosis as is demonstrated by an increase in caspase 3/7 activity after 48 hours of treatment with different doses of AZD4547 in a panel of MPM cell lines. (**E**) FGFR inhibitor PD173074 kills mesothelioma cell lines via induction of apoptosis as is demonstrated by an increase in caspase 3/7 activity after 48 hours of treatment with different doses of PD-173074 a panel of MPM cell lines.

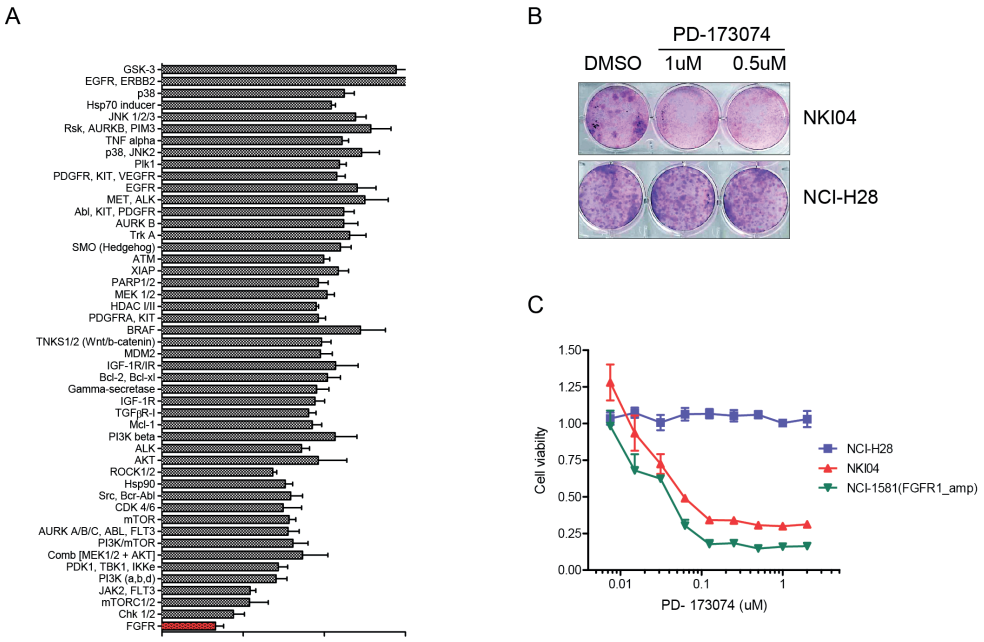

Figure 2. Sensitivity to FGFR inhibitors in primary mesothelioma lines.

(**A**) Cell viability (mean ±SD) of primary mesothelioma line NKI04 after treatment with a fixed does of 48 different small molecule inhibitors. This cell line is most sensitive to FGFR inhibition. (**B**) Fourteen-day clonogenic survival assay of primary mesothelioma line NKI04 compared with immortalized mesothelioma line NCI-H28 treated with FGFR inhibitor PD-173074 at concentrations of 500 nmol/L and 1 mmol/L. (**C**) Cell viability (mean ±SD) of primary mesothelioma line NKI04 compared with immortalized mesothelioma line NCI-H28 and FGFR-dependent lung cancer cell line NCI-H1581 (y-axis), as a function of the concentration of FGFR inhibitor PD-173074.

family genes was correlated with sensitivity to PD-173074 to explore whether the variation in any single family member, either ligand or receptor, was associated with response to FGFR inhibition. We found a statistically significant correlation between elevated FGF9 mRNA expression and response to PD-173074 (P=0.0148) and AZD4547 treatment (P=0.0098; Fig. 3A). FGF9 is a secreted, high-affinity ligand for the FGFR3 receptor, with low affinity for the FGFR1 and FGFR2 receptors (19). To determine whether a subset of MPM exhibits elevated expression of the FGF9 ligand in patients, we analyzed gene expression from a panel of 53 assorted MPM and matched normal lung clinical samples (Fig. 3B; ref. 20). Overall, we observed significantly higher FGF9 transcript levels in MPM tumors compared with pleura and lung normal tissue (P< 0.0001). Therefore, similar to our observation in the MPM cell lines, a subset of patient samples also demonstrates high levels of FGF9 expression.

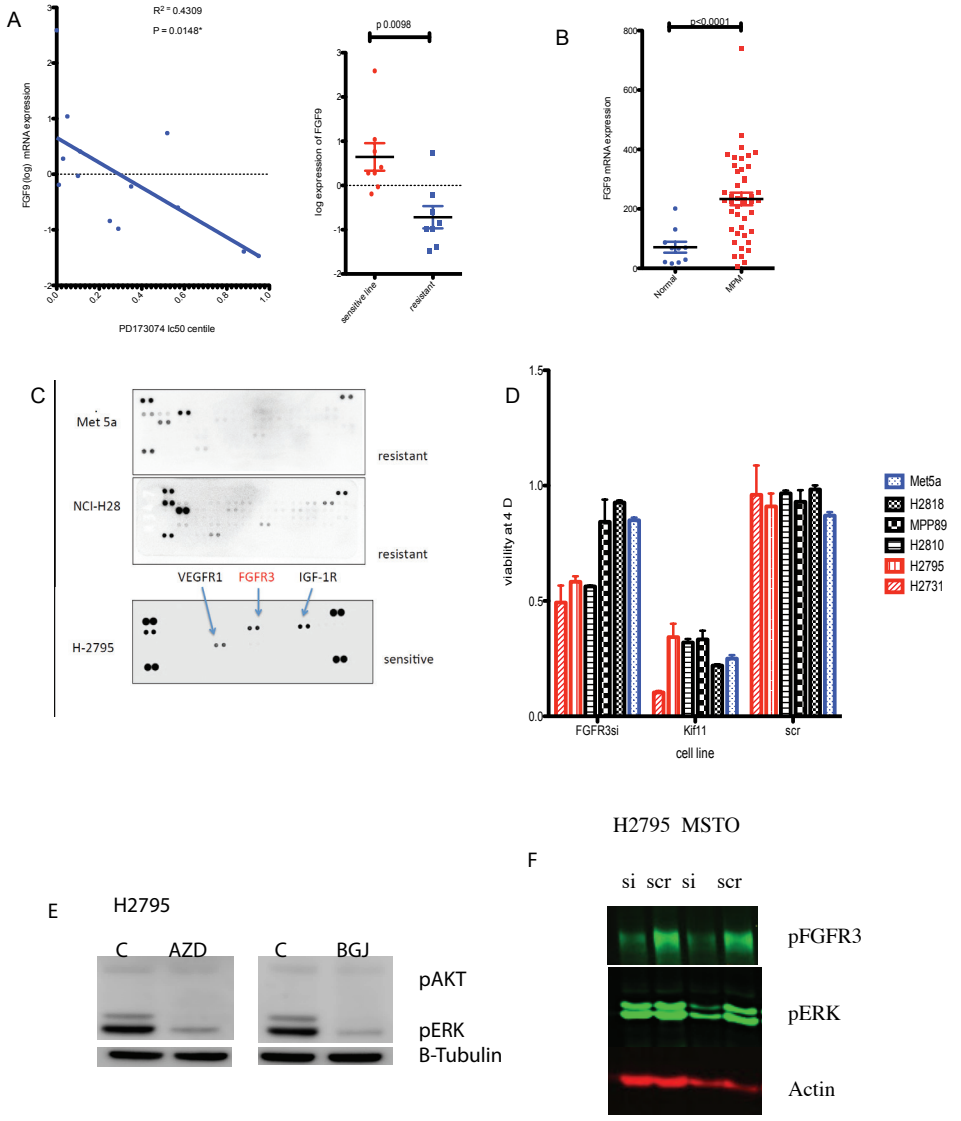

Figure 3. FGFR inhibitor sensitivity is mediated by FGF axis signaling through FGF9 and FGFR3.

(**A**) Scatterplot depicting sensitivity to FGFR inhibitor PD-173074 as a function of expression of FGF9. mRNA. Y-axis depicting log mRNA expression of FGF9 and x-axis showing centile of IC_{50} to PD173074 of individual MPM cell line in cell line screen. High FGF9 gene expression is significantly correlated to high sensitivity to FGFR inhibition. Right hand scatterplot showing FGF9 expression correlates with sensitivity to AZD4547. (**B**) Expression of FGF9 in a set of MPM tumors, compared with normal lung and pleura, derived from GE0 dataset GSE2549. The mean expression in MPM tumors is significantly higher than that of normal lung and pleura. (**C**) Phospho-RTK array reveals phosphorylated-FGFR3 in FGFR inhibitor–sensitive cell line H2795 that is absent in two resistant lines (NCI-H28 and Met5a). (**D**) Cell viability of MPM cell lines after silencing of the FGFR3 transcript demonstrates reduced viability of FGFR inhibitor–sensitive cell lines H2795, H2810, and H2731 compared with FGFR inhibitor–resistant lines Met5A, NCI-H2052, H2818, and MPP89. Viability at 4 days post transfection is compared with Kif11–positive control siRNA and scrambled negative control. (**E**) Modulation of pERK signaling in H2795 cell line following 6 hours of exposure to DMSO (C) or 500 nmol/L AZD4547 or DMSO and 100 nmol/L BGJ398. (**F**) siRNA-mediated knockdown of pFGFR3 in H2795 and MSTO211H, showing effect on pFGFR3 and pERK versus scrambled control.

Modulation of FGF/FGFR function in MPM lines

A possible premise for the observed sensitivity of MPM lines that express high levels of FGF9 would be activation of the FGFR3 receptor kinase in an autocrine loop and subsequent engagement of prosurvival downstream signaling pathways. Indeed, a comparison of phosphorylation status of 42 receptor tyrosine kinases between a small sample of MPM cell lines demonstrated increased phosphorylation of FGFR3 in the sensitive line H2795 but not in resistant lines Met-5A and NCI-H28 (Fig. 3C).

To further confirm a critical role for FGFR3, this transcript was silenced by siRNA in a panel of MPM cell lines and the direct effect on cell viability was measured. Transient siRNA-mediated silencing of the FGFR3 transcript reduced cell viability in all 3 FGFR inhibitor-sensitive cell lines, but not in the FGFR inhibitor-resistant lines. This indicates a dependency on FGFR3 mediated signaling of the FGFR inhibitor-sensitive lines (Fig. 3D). As would be expected, inhibition of FGFR3 by the specific inhibitors AZD4547 and BJG398 decreased pERK levels (Fig. 3E), and this was also seen following siRNA-mediated silencing of FGFR3 in H2795 and MSTO-211H (Fig. 3F). The addition of the FGF9 ligand to MPM cells lacking baseline FGFR3 activation was able to induce phosphorylation of FGFR3 and a change in the growth kinetics of this cell line in a dose-dependent fashion (Supplementary Fig. S5).

Role of BAP1 in modulating FGF pathway signaling

Although we failed to identify genomic alterations in any member of the FGFR family that might explain the sensitivity to FGFR inhibition, we reasoned that this dependency might also be the consequence of other gene aberrations up- or downstream of FGFR3 signaling. We evaluated the gene expression and mutation database for other statistical associations explaining sensitivity to the FGFR inhibitor AZD4547 in the panel of MPM cell lines. We focused on driver mutations or copy-number alterations in three of the most frequently mutated genes in MPM, namely BAP1, NF2, and CDKN2A (7). We detected a weak but non-significant association between AZD4547 sensitivity and BAP1 mutations in the sensitive cell lines (Fig. 4A). Given that loss of BAP1 protein expression might also occur through nonmutational mechanisms as previously described (21), we additionally characterized BAP1 protein status in these lines by Western blot analysis (Supplementary Figs. S3 and S4). When sensitivity to the AZD4547 was correlated with BAP1 protein expression (low/absent vs. expressed), there was a significant correlation between loss of BAP1 expression and sensitivity (P=0.0208; Fig. 4B).

Functional consequences of BAP1 modulation on FGFR signaling.

Because silencing FGFR3 reduced cell viability in a subset of MPM lines, we next investigated whether this dependency on FGFR signaling was regulated by BAP1. BAP1 is a nuclear deubiquitinating enzyme with many unelucidated functions that might include modulation of the FGFR pathway. Silencing of BAP1 expression resulted in increased phosphorylation

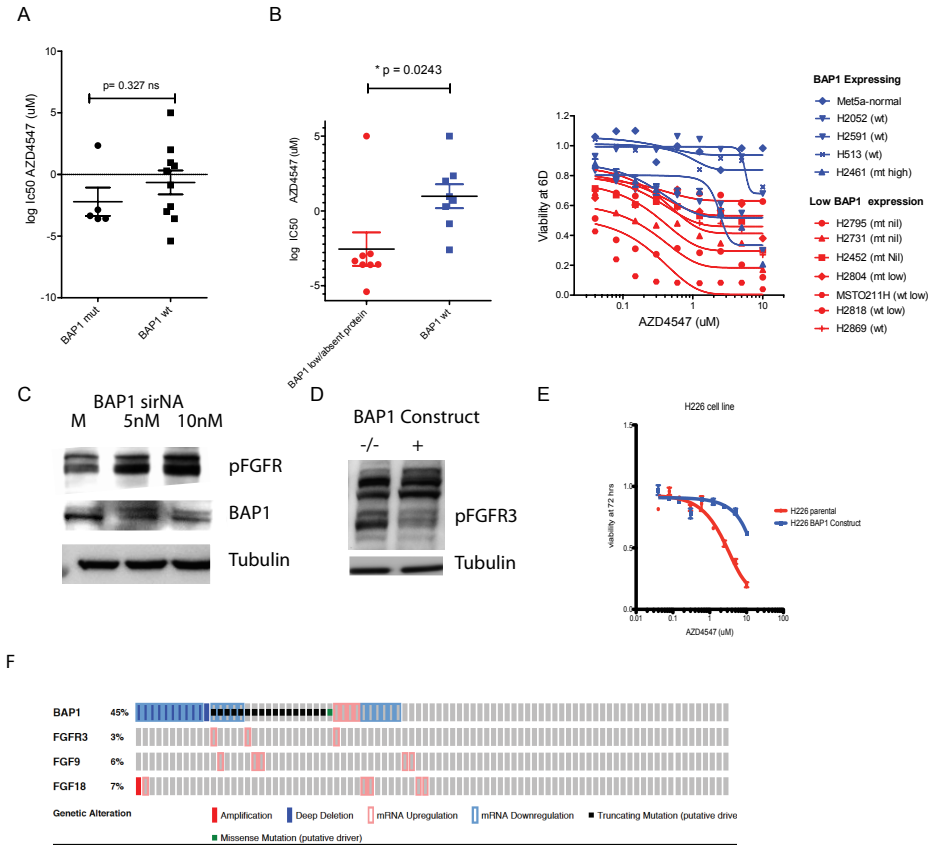

Figure 4 Loss of BAP1 protein expression is correlated to FGFR inhibitor sensitivity.

(**A**) Sensitivity to FGFR inhibitor AZD4547—expressed as logIC50 value—of cell lines, grouped according to BAP1 mutation status. The mean logIC50 value is not significantly different between the two groups. (**B**) Sensitivity to FGFR inhibitor AZD4547 according to BAP1 protein expression. Red are cell lines with low or absent BAP1 protein. Blue lines have normal BAP1 protein expression. Sensitivity (left) is expressed as logIC50 value (y-axis). The difference between the two groups is statistically significant. Cell viability (right) of different mesothelioma lines (y-axis) after treatment with FGFR inhibitor AZD4547 (x-axis). wt, wild-type; mt, mutant; high, high protein expression; low, low protein expression; nil, no protein expression. Right-hand panel showing dose–response curves of MPM cell lines treated with FGFR inhibitor AZD4547. Cell lines in red are lines with low or absent BAP1 protein expression. Blue lines have normal BAP1 protein expression. (**C**) SiRNA-mediated depletion of BAP1 in H2052 at increasing siRNA doses of 5 and 10 nmol/L versus mock transfected (M) control. Western blot comparing pFGFR3 and BAP1 expression at these conditions. Tubulin as loading control. (**D**) BAP1 overexpression in BAP1-null cell line H226. Western blot of BAP1 construct versus parental cell line baseline pFGFR levels with tubulin as loading control. (**E**) Cell viability after treatment with increasing doses of FGFR inhibitor AZD4547 in parental cell line H226 BAP1-null (red) and in the same cell line with BAP1 construct (red). BAP1 overexpression increases cell viability after FGFR inhibition. (**F**) Co-occurence of somatic mutations in BAP1 and FGFR family members in MPM tumors in the TCGA cohort.

of FGFR3 (Fig. 4C). Conversely, restoring BAP1 expression in the BAP1-null MPM line (Fig. 4D) H226 resulted in a decrease in pFGFR and a modest increase in resistance to the FGFR inhibitor AZD4547 (Fig. 4E).

We observed increased expression at the protein level in the BAP1 mutant cell lines of other RTK receptor genes and their appropriate ligands also known to be important in cell survival signaling in MPM such as PDGFRB, IGF1-R, and MET (22) using phospho-RTK arrays (Supplementary Fig. S4A and S4B). The H226-null MPM cell line was transfected with a wild-type BAP1 construct and a functionally inactive C91A-mutant BAP1 construct. Gene expression analysis on these two lines was performed and Signaling Pathway Impact Analysis (SPIA) of the data (Supplementary Table S) demonstrated that among the most significantly activated pathways in BAP1-inactive cells is the "Bladder Cancer" pathway including FGFR3 (arrow, Supplementary Fig. S6A) illustrated in Supplementary Figure S6B (23). In summary, the gene expression analysis demonstrates that BAP1 loss of function is associated with a transcriptional response upregulating not only FGFR signaling but also other RTKs such as PDGFRB, CMET, and IGF1R, that may be important mediators of cell growth and survival. However, only FGFR inhibitors showed a significant viability effect as single agents. We analyzed gene expression data from a study of 51 mesothelioma tumor samples to see if a similar effect on the FGFR pathway was seen *in vivo* (40 BAP1 wild-type and 11 mutant; GEO GSE29354; ref. 24). Amongst members of the FGFR signaling family, BAP1-mutant tumors did indeed demonstrate increased expression of FGF18, FGFR2, and FGFR3 relative to BAP1 wild-type tumors (Supplementary Table). To explore this association further in human tumors, we analyzed the available TCGA data and looked for the incidence of genetic and mRNA alterations of these genes in MPM tumors by BAP1 status (Fig. 4F). This showed the majority of dysregulation (10 of 14) events in FGF9, FGF18, and FGFR3 occurred in the context of BAP1 gene or mRNA dysregulation.

FGFR inhibition in MPM xenograft model

To assess the in vivo efficacy of targeting FGFR in MPM, we established a xenograft model using the FGFR inhibitor-sensitive MPM lines H2795 and MSTO-211H. Mice were treated with AZD4547, a selective inhibitor of FGFR1/2/3, which is currently being evaluated in clinical trials. We observed that treatment with AZD4547 resulted in significant growth inhibition in the H2795- and MSTO-211H-derived tumors (Fig. 5A). Furthermore, AZD45457 treated tumors showed a reduction in pERK signaling by immunohistochemistry compared with vehicle control-treated tumors (Fig. 5B), indicating target engagement by the drug in this model. Caspase activation was also seen in drug-treated tumors suggesting apoptosis (Supplementary Fig. S7).

Combination therapeutic screen

As the single-agent efficacy of FGFR inhibition was seen only in a subset of MPM cell lines, and because persistent pAKT pathway activation was seen in cell lines not responsive to FGFR inhibition, we hypothesized that a combination screen utilizing a PI3 Kinase inhibitor may reveal useful synergies. We undertook an anchor-based combination screen in 15 MPM cell lines using 95 small-molecule inhibitors (see Supplementary Table for details) selected

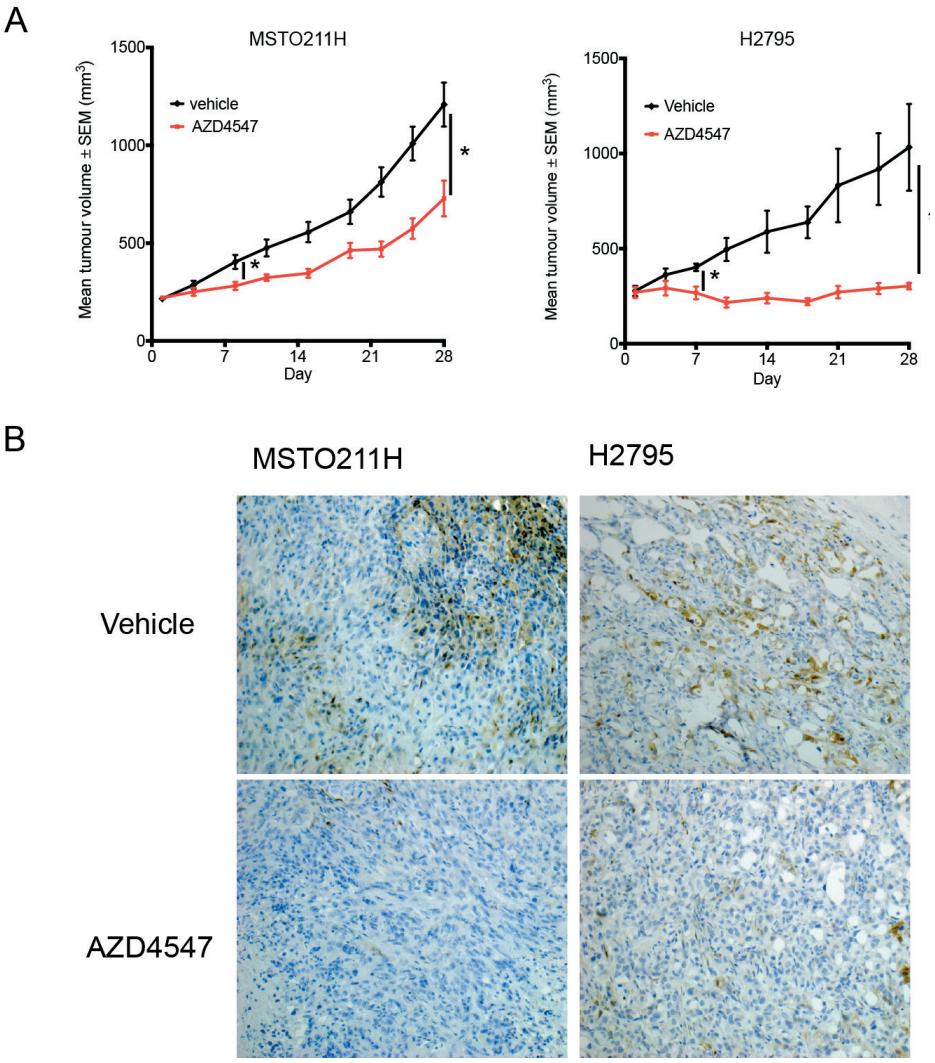

Figure 5. Xenograft mouse model shows FGFR inhibition efficacy in vivo.

(**A**) Xenograft mouse model using mesothelioma cell lines H2795 and MSTO211H. Mean tumor volume is depicted on the y-axis as a function of time (x-axis). Red lines indicate tumor growth in mice treated with FGFR inhibitor AZD4547, while the black lines indicate growth in vehicle-treated mice. (**B**) Immunohistochemistry of AZD4547- versus vehicle control-treated xenograft tumors. ppERK expression in representative tumors in drug-treated versus vehicle control groups.

to target many critical pathways in cancer, both as single agents and in combination with a fixed dose of the PI3 Kinase inhibitor AZD6482. The resulting difference in area under the curve (AUC) between single agent small-molecule inhibitor and the combination with AZD6482 was used to calculate synergy. The most recurrent synergistic interactions were seen with IGF1R inhibitor BMS-536924 and FGFR inhibitor PD-173074 (Supplementary Fig.

S8A) with synergy observed in seven and six of 15 lines, respectively. Supplementary Fig. S8B shows a validation dose-response curve of the FGFRi-resistant NCI H28 cell lines showing minimal effect of BMS 536824 or AZD6482 alone, but reduced viability and pAKT reduction with the combination. This cytotoxicity is not seen in the mesothelial control cell line Met5a, suggesting that the synergy is not generic but cell line specific.

Discussion

Because MPM is a rare and heterogeneous tumor, it is notoriously difficult to identify and characterize responding subgroups in clinical trials. Our work illustrates the application and possibilities of comprehensive pharmacogenomic profiling approaches in intractable cancers such as MPM. The finding of FGFR inhibitor sensitivity in a subgroup of immortalized MPM cell lines represents a potentially novel therapeutic approach for this tumor type. As immortalized cell lines may undergo genetic drift, we also confirmed our findings in primary mesothelioma early-passage lines.

Dysregulation of the FGFR pathway has been described in many cancer types (25, 26). FGF9 signaling through FGFR3 has been shown to have a role in the development and progression of tumor cells in mouse models for NSCLC and prostate cancer (27). In MPM cell line models, we observed that high levels of the ligand FGF9 were strongly correlated with sensitivity to the FGFR inhibitor PD-173074 and AZD4547. We hypothesize that the effects of FGF9 are mediated through FGFR3 signaling, as illustrated by modulation of downstream ERK phosphorylation upon chemical inhibition with small-molecule inhibitors of FGFR3 and knockdown of FGFR3. FGFR3 is conversely not phosphorylated in cell lines insensitive to FGFRi, and this phosphorylation can be induced by the addition of synthetic FGF9 ligand. Interestingly, there was variability in FGF9 mRNA expression levels among the MPM cell lines, similar to what is observed in tumors in previously published studies. Recently, other groups demonstrated efficacy of FGFR inhibition in preclinical models of MPM mediated by other FGF-pathway members such as FGFR1 (18, 28, 29). We confirm the efficacy of a clinically utilized FGFR inhibitor including AZD4547 *in vivo* in MPM xenograft models. Furthermore, since undertaking these studies, early-phase clinical work with pharmacokinetic data has been published (30, 31) on AZD4547 and BGJ398. These have confirmed that the doses used in the *in vitro* work (100 nmol/L to 1 μmol/L) here are achievable in plasma *in vivo* and are able to modulate the target, with pharmacodynamic end points of target engagement with FRS2 downregulation and changes in serum phosphate levels seen.

FGF-receptors and -ligands are being targeted in clinical trials by both selective and nonselective FGFR TKI's and monoclonal antibodies (32) and AZD4547 has shown modest clinical activity in tumors with FGFR-pathway aberrant activation (33). In MPM dovitinib, a

multitargeting kinase inhibitor with activity against FGFR has been trialed and has failed in small cohort of patients with MPM (34). Because the data across tumor types demonstrate only a small group of patients responds to FGFR inhibition, it is crucial to find biomarkers that predict response to FGFR inhibition. Guagnano et al. integrated genomic and transcriptomic data of about 500 tumor cell lines with drug-sensitivity data to find predictive biomarkers for response to FGFR inhibitor NVP-BGJ398. A genetic alteration in one of the four FGF-receptors was found in 7% of cell lines, but only about half of the cell lines with such an alteration was found to be sensitive (35).

We did not find any mutation, amplification, or fusion transcripts of the FGFR-family in the inhibitor-sensitive MPM cell lines. The genes that were most recurrently altered in our MPM cell lines include CDKN2A, BAP1, and NF2. The frequency at which these genes were mutated is broadly similar to those previously described in clinical MPM samples (6, 7).

We show that loss of BAP1 expression was associated with sensitivity to FGFR inhibition. This finding was further validated with modulation of pFGFR-signaling and dose-response kinetics to FGFR inhibition following siRNA-mediated knockdown and BAP1 overexpression in MPM cell lines. Caveats with this association were also observed: NCI-H28 was one of the most resistant cell lines to FGFR inhibition but carried a BAP1 homozygous deletion, suggesting that BAP1 loss may enrich for FGFR inhibitor-sensitive cell lines but that some heterogeneity of drug response may still be observed. BAP1 (BRCA-associated protein 1) is a nuclear deubiquinating enzyme that controls gene expression by interaction with numerous transcription factors and other complexes, including those of the double strand DNA-break repair machinery (36). BAP1 thus influences cell-cycle progression (37) and double-strand DNA break repair (38). We show here that its loss may also affect gene expression of FGF pathway members, thereby enhancing signaling through this pathway.

The BAP1 gene is inactivated by somatic mutation in 23% to 64% of patients with MPM and between 1% and 47% in other tumor types (24, 39-43). Furthermore, BAP1 protein levels are undetectable in about 25% of MPM with normal BAP1 gene status, likely by epigenetic modification (24). BAP1 loss was observed to enrich for FGFR inhibitor-sensitive MPM lines, and expression of C91 hydrolase inactive mutant versus wild-type BAP1 protein in the H226 cell line induced activation of FGFR3 signaling. We hypothesize that inactivation of BAP1 in MPM, possibly through its function as a ubiquitin hydrolase, induces changes in gene expression of both FGF-family ligands and receptors to stimulate cell growth and survival.

We performed a combination drug screen to assess the impact of novel combinations of targeted therapies on MPM cell lines. On the 15 MPM cell lines screened, we found that FGFR and IGF1R inhibitors were the most recurrently synergistic with the PI3-Kinase inhibitor AZD6482. This is the first time, to our knowledge, that both a single agent and

combination therapeutic screen have been performed, which point to the primacy of the FGFR signaling pathway in MPM. Interestingly, one of the most resistant cell lines to FGFR inhibition was amenable to treatment with AZD6482 plus IGF1R inhibition with evidence of ablation of pAKT with the combination of drugs but not with either alone, implying true synergy. Previous studies have identified that multiple RTK's are active in MPM (14), and this has provided some rationale to consider combination therapies to overcome innate resistance to targeted therapies. It is also interesting to speculate as to whether IGF1R plus Pi3K inhibition would be of use in acquired resistance to FGFR inhibitors.

Conclusion

High-throughput drug screening revealed a subset of both immortalized and primary mesothelioma cell lines to be highly sensitive to FGFR inhibition. This sensitivity was mediated through FGFR3 and was associated with loss of BAP1 protein expression. The high incidence of BAP1 protein loss in MPM tumors implies potential benefit from FGFR inhibition for a substantial subset of this patient group. In addition, our anchor-based screens revealed synergistic combinations that helped to overcome innate resistance to FGFR inhibition.

References

1. van Meerbeeck JP, Scherpereel A, Surmont VF, Baas P. Malignant pleural mesothelioma: the standard of care and challenges for future management. Crit Rev Oncol Hematol 2011;78:92–111.
2. Frank AL, Joshi TK. The global spread of asbestos. Ann Glob Health 2014;80:257–62.
3. Baas P, Fennell D, Kerr KM, Van Schil PE, Haas RL, Peters S, et al. Malignant pleural mesothelioma: ESMO clinical practice guidelines for diagnosis, treatment and follow-up. Ann Oncol 2015;26:v31–v39.
4. Vogelzang NJ, Rusthoven JJ, Symanowski J, Denham C, Kaukel E, Ruffie P, et al. Phase III study of pemetrexed in combination with cisplatin versus cisplatin alone in patients with malignant pleural mesothelioma. J Clin Oncol 2003;21:2636–44.
5. Pinton G, Manente AG, Tavian D, Moro L, Mutti L. Therapies currently in phase II trials for malignant pleural mesothelioma. Expert Opin Investig Drugs 2013;22:1255–63.
6. Ladanyi M, Zauderer MG, Krug LM, Ito T, McMillan R, Bott M, et al. New strategies in pleural mesothelioma: BAP1 and NF2 as novel targets for therapeutic development and risk assessment. Clin Cancer Res 2012;18: 4485–90.
7. Bueno R, Stawiski EW, Goldstein LD, Durinck S, De Rienzo A, Modrusan Z, et al. Comprehensive genomic analysis of malignant pleural meso- thelioma identifies recurrent mutations, gene fusions and splicing alterations. Nat Genet 2016;48:407–16.
8. Shapiro IM, Kolev VN, Vidal CM, Kadariya Y, Ring JE, Wright Q, et al. Merlin deficiency predicts FAK inhibitor sensitivity: a synthetic lethal relationship. Sci Transl Med 2014;6:237ra68.
9. Govindan R, Kratzke RA, Herndon JE 2nd, Niehans GA, Vollmer R, Watson D, et al. Gefitinib in patients with malignant mesothelioma: a phase II study by the Cancer and Leukemia Group B. Clin Cancer Res 2005;11:2300–4.
10. Mathy A, Baas P, Dalesio O, van Zandwijk N. Limited efficacy of imatinib mesylate in malignant mesothelioma: a phase II trial. Lung Cancer 2005;50:83–6.
11. Baas P, Boogerd W, Dalesio O, Haringhuizen A, Custers F, van Zandwijk N. Thalidomide in patients with malignant pleural mesothelioma. Lung Cancer 2005;48:291–6.
12. Fennell DA, McDowell C, Busacca S, Webb G, Moulton B, Cakana A, et al. Phase II clinical trial of first or second-line treatment with bortezomib in patients with malignant pleural mesothelioma. J Thorac Oncol 2012;7: 1466–70.
13. Krug LM, Kindler HL, Calvert H, Manegold C, Tsao AS, Fennell D, et al. Vorinostat in patients with advanced malignant pleural mesothelioma who have progressed on previous chemotherapy (VANTAGE-014): a phase 3, double-blind, randomised, placebo-controlled trial. Lancet Oncol 2015;16:447–56.
14. Menges CW, Chen Y, Mossman BT, Chernoff J, Yeung AT, Testa JR. A phosphotyrosine proteomic screen identifies multiple tyrosine kinase signaling pathways aberrantly activated in malignant mesothelioma. Genes Cancer 2010;1:493–505.

15. Irizarry RA, Hobbs B, Collin F, Beazer-Barclay YD, Antonellis KJ, Scherf U, et al. Exploration, normalization, and summaries of high-density oligo- nucleotide array probe level data. Biostatistics 2003;4:249–64.
16. Hanzelmann S, Castelo R, Guinney J. GSVA: gene set variation analysis for microarray and RNA-seq data. BMC Bioinformatics 2013;14:1471–2105.
17. Iorio F, Knijnenburg TA, Vis DJ, Bignell GR, Menden MP, Schubert M, et al. A landscape of pharmacogenomic interactions in cancer. Cell 2016;166: 740–754.
18. Marek LA, Hinz TK, von M€assenhausen A, Olszewski KA, Kleczko EK, Boehm D, et al. Nonamplified FGFR1 is a growth driver in malignant pleural mesothelioma. Mol Cancer Res 2014;12:1460–9.
19. Zhang X, Ibrahimi OA, Olsen SK, Umemori H, Mohammadi M, Ornitz DM. Receptor specificity of the fibroblast growth factor family. The complete mammalian FGF family. J Biol Chem 2006;281:15694–700.
20. Gordon GJ, Rockwell GN, Jensen RV, Rheinwald JG, Glickman JN, Aronson JP, et al. Identification of novel candidate oncogenes and tumor suppres- sors in malignant pleural mesothelioma using large-scale transcriptional profiling. Am J Pathol 2005;166:1827–40.
21. Shah AA, Bourne TD, Murali R. BAP1 protein loss by immunohistochem- istry: a potentially useful tool for prognostic prediction in patients with uveal melanoma. Pathology 2013;45:651–6.
22. Brevet M, Shimizu S, Bott MJ, Shukla N, Zhou Q, Olshen AB, et al. Coactivation of receptor tyrosine kinases in malignant mesothelioma as a rationale for combination targeted therapy. J Thorac Oncol 2011;6:864–74.
23. Tarca AL, Draghici S, Khatri P, Hassan SS, Mittal P, Kim JS, et al. A novel signaling pathway impact analysis. Bioinformatics 2009;25:75–82.
24. Bott M, Brevet M, Taylor BS, Shimizu S, Ito T, Wang L, et al. The nuclear deubiquitinase BAP1 is commonly inactivated by somatic mutations and 3p21.1 losses in malignant pleural mesothelioma. Nat Genet 2011;43:668–72.
25. Dienstmann R, Rodon J, Prat A, Perez-Garcia J, Adamo B, Felip E, et al. Genomic aberrations in the FGFR pathway: opportunities for targeted therapies in solid tumors. Ann Oncol 2014;25:552–63.
26. Helsten T, Elkin S, Arthur E, Tomson BN, Carter J, Kurzrock R. The FGFR landscape in cancer: analysis of 4,853 tumors by next-generation sequenc- ing. Clin Cancer Res 2016;22:259–67.
27. Suzuki T, Yasuda H, Funaishi K, Arai D, Ishioka K, Ohgino K, et al. Multiple roles of extracellular fibroblast growth factors in lung cancer cells. Int J Oncol 2015;46:423–9.
28. Schelch K, Hoda MA, Klikovits T, Mu€nzker J, Ghanim B, Wagner C, et al. Fibroblast growth factor receptor inhibition is active against mesothelioma and synergizes with radio- and chemotherapy. Am J Respir Crit Care Med 2014;190:763–72.

29. Plones T, Beckers F, Engel-Riedel W, Stoelben E, Brockmann M, Schildgen V, et al. Absence of amplification of the FGFR1-gene in human malignant mesothelioma of the pleura: a pilot study. BMC Res Notes 2014;7:549.
30. Nogova L, Sequist LV, Perez Garcia JM, Andre F, Delord JP, Hidalgo M, et al. Evaluation of BGJ398, a fibroblast growth factor receptor 1-3 kinase inhibitor, in patients with advanced solid tumors harboring genetic alterations in fibroblast growth factor receptors: results of a global phase I, dose-escalation and dose-expansion study. J Clin Oncol 2017;35:157–165.
31. Gavine PR, Mooney L, Kilgour E, Thomas AP, Al-Kadhimi K, Beck S, et al. AZD4547: an orally bioavailable, potent, and selective inhibitor of the fibroblast growth factor receptor tyrosine kinase family. Cancer Res 2012;72:2045–56.
32. Touat M, Ileana E, Postel-Vinay S, Andr'e F, Soria JC. Targeting FGFR signaling in cancer. Clin Cancer Res 2015;21:2684–94.
33. Paik PK, Shen R, Berger MF, Ferry D, Soria JC, Mathewson A, et al. A phase Ib open-label multicenter study of AZD4547 in patients with advanced squamous cell lung cancers. Clin Cancer Res 2017;23: 5366–5373.
34. Laurie SA, Hao D, Leighl NB, Goffin J, Khomani A, Gupta A, et al. A phase II trial of dovitinib in previously-treated advanced pleural meso- thelioma: the Ontario clinical oncology group. Lung Cancer 2017;104:65–69.
35. Guagnano V, Kauffmann A, Wo€hrle S, Stamm C, Ito M, Barys L, et al. FGFR genetic alterations predict for sensitivity to NVP-BGJ398, a selective pan- FGFR inhibitor. Cancer Discov 2012;2:1118–33.
36. Yu H, Mashtalir N, Daou S, Hammond-Martel I, Ross J, Sui G, et al. The ubiquitin carboxyl hydrolase BAP1 forms a ternary complex with YY1 and HCF-1 and is a critical regulator of gene expression. Mol Cell Biol 2010;30:5071–85.
37. Eletr ZM, Wilkinson KD. An emerging model for BAP1^{0} s role in regulating cell cycle progression. Cell Biochem Biophys 2011;60:3–11.
38. Yu H, Pak H, Hammond-Martel I, Ghram M, Rodrigue A, Daou S, et al. Tumor suppressor and deubiquitinase BAP1 promotes DNA double-strand break repair. Proc Natl Acad Sci U S A 2014;111:285–90.
39. Yoshikawa Y, Sato A, Tsujimura T, Emi M, Morinaga T, Fukuoka K, et al. Frequent inactivation of the BAP1 gene in epithelioid-type malignant mesothelioma. Cancer Sci 2012;103:868–74.
40. Nasu M, Emi M, Pastorino S, Tanji M, Powers A, Luk H, et al. High Incidence of Somatic BAP1 alterations in sporadic malignant mesotheli- oma. J Thorac Oncol 2015;10:565–76.
41. Murali R, Wiesner T, Scolyer RA. Tumours associated with BAP1 mutations. Pathology 2013;45:116–26.
42. Lu C, Zhang J, Nagahawatte P, Easton J, Lee S, Liu Z, et al. The genomic landscape of childhood and adolescent melanoma. J Invest Dermatol 2015;135:816–23.

43. Carbone M, Flores EG, Emi M, Johnson TA, Tsunoda T, Behner D, et al. Combined genetic and genealogic studies uncover a large BAP1 cancer syndrome kindred tracing back nine generations to a common ancestor from the 1700s. PLoS Genet 2015;11:e1005633

Supplemental Data

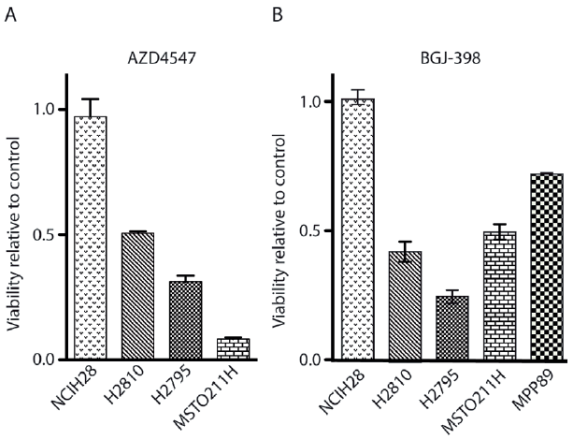

Figure. S1. A subset of MPM cell lines respond to FGFR inhibition.

Cell viability of selected mesothelioma cell lines (NCI-H28, H2810, H2795, MSTO-211H and MPP-89) after 72 hours of treatment with (A) AZD4547 at a fixed dose of 500 nmol/L and (B) BGJ398 at a fixed dose of 300 nmol/L

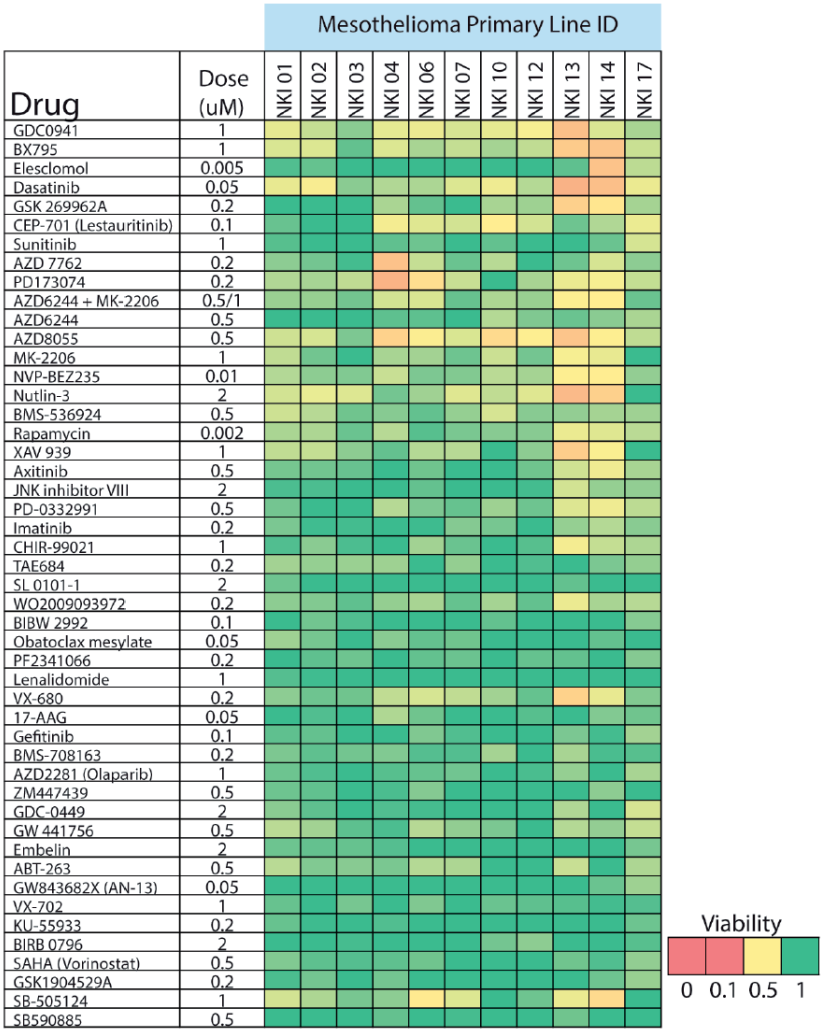

Figure. S2. A subset of pleural fluid derived early passage primary cultures (EPL) respond to FGFR inhibition.

Cell viability of 11 early passage primary cultures (columns) after treatment with a fixed dose of 48 small molecule inhibitors (rows), depicted in a color scale (green: 100% cell viability; red: 0% cell viability).

A

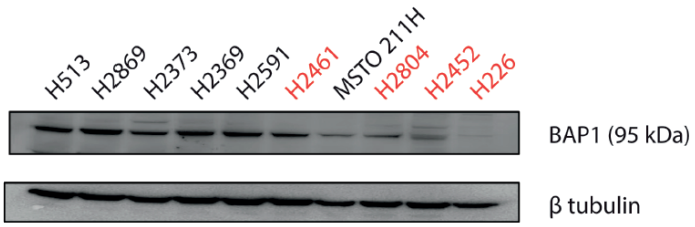

B

Cell line	CHR	GENE_NAME	CDS_SYNTAX	AA_MUT_SYN	Class	DESCRIPTION
H2461	3	BAP1	c.65delT	p.F22fs*50	indel	Deletion - Frameshift
H2722	3	BAP1	c.?	p.0	indel	HomDel
H2731	3	BAP1	c.123-15_131(	p.?	indel	Essential Splice
H2795	3	BAP1	c.38-7_49del1	p.?	indel	Essential Splice
H2804	3	BAP1	c.37+4_37+5in	p.?	indel	Essential Splice
IST-MES1	3	BAP1	c.1983+1_198	p.?	indel	Essential Splice
NCI-H2452	3	BAP1	c.284C>A	p.A95D	Missense	Substitution - Missense
NCI-H28	3	BAP1	c.438-19_441(	p.?	indel	Essential Splice

Figure. S3. BAP1 mutation status does not correlate fully with protein expression.

(A) Western Blot showing BAP1 protein expression in several MPM cell lines, both BAP1 wild type (black) and mutant lines (red). Beta-tubulin represents the protein loading control. (B) List of somatic mutations in BAP1 seen in MPM cell lines.

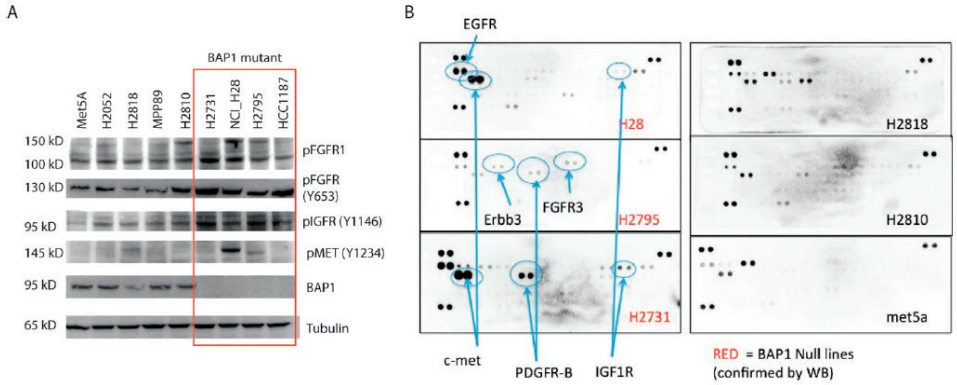

Figure. S4. BAP1 null cell lines show increased activity of multiple tyrosine kinases.

(A) Western Blot showing BAP1 protein expression in several MPM cell lines as well as activation in IGFR, MET and FGFR. (B) Phospho-RTK array panel showing baseline RTK-activation of BAP1 mutant (highlighted in red) versus wild type mesothelioma cell lines.

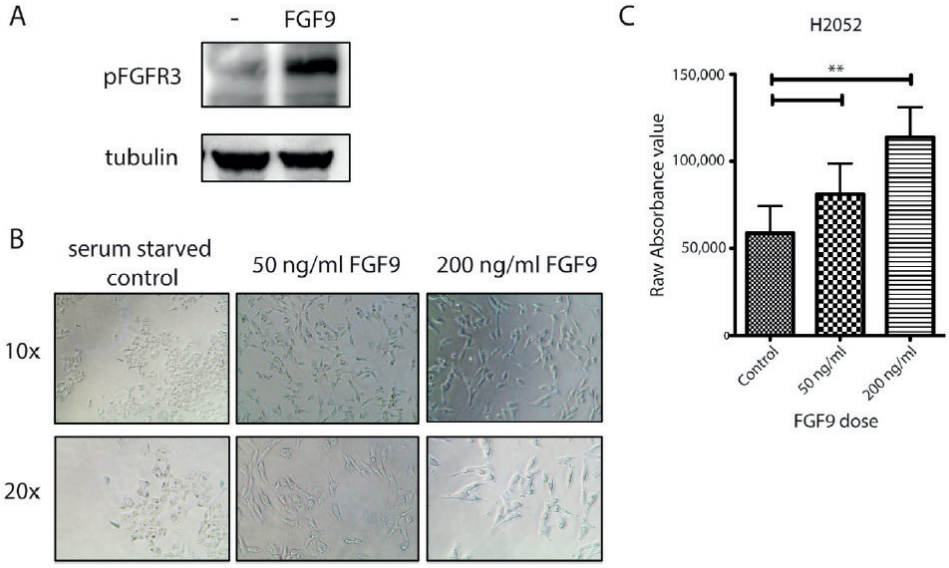

Figure. S5. FGF9 activated FGFR3 modulates growth and phenotype.

(A) Western Blot of pFGFR in serum-starved H2052 MPM cell line at baseline and following the addition of recombinant FGFR9 ligand (50 ng/mL) after 1 hour. (B) Light microscopy at 10x and 20x magnification of H2052 cell line under serum-starved conditions and with the addition of FGF9 ligand at 2 concentrations. (C) Comparative viability of H2052 by SYTO60 assay at baseline and following the addition of FGF9 ligand at 50ng/mL and 200ng/mL.

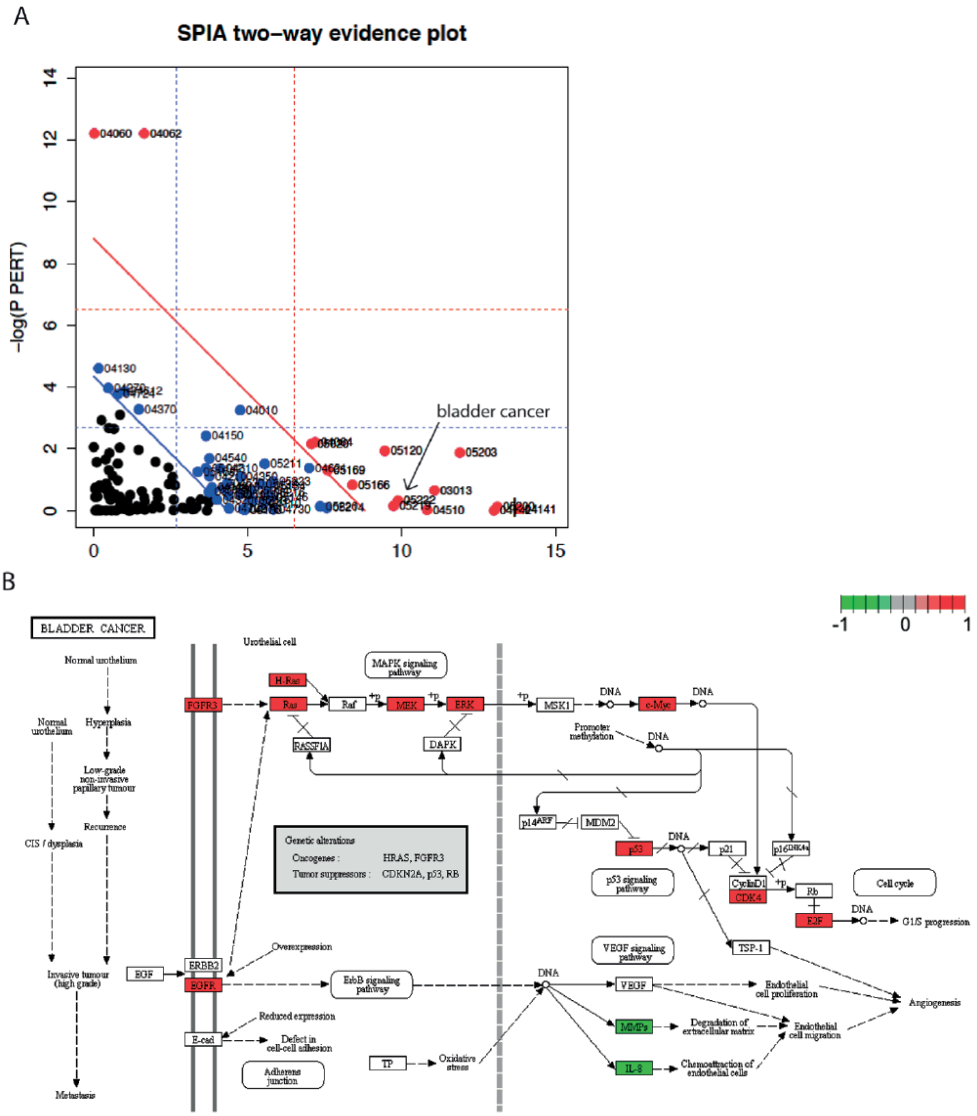

Figure. S6. BAP1 modulation and FGFR pathway activation by gene expression.

(A) Gene expression analysis of H226 cell line (BAP1 null) transfected with wild type BAP1 construct versus BAP1 inactive (C91A) construct. SPIA pathway analysis of C91A versus wild type cell line revealed the KEGG 'bladder cancer' pathway to be significantly activated in C91A cell line. (B) 'Bladder cancer' pathway showing genes that are overexpressed in the C91A line in red.

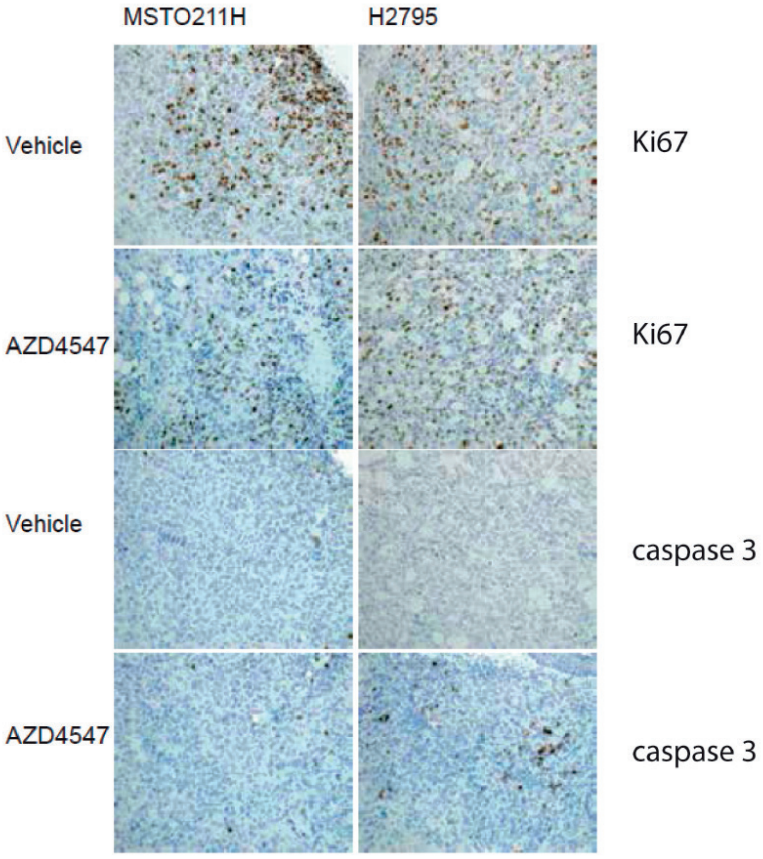

Figure. S7. Xenograft tumor immunohistochemistry.

Immunohistochemistry for Caspase3 and Ki67 in MPM xenograft tumors AZD4547-treated conditions compared to vehicle control.

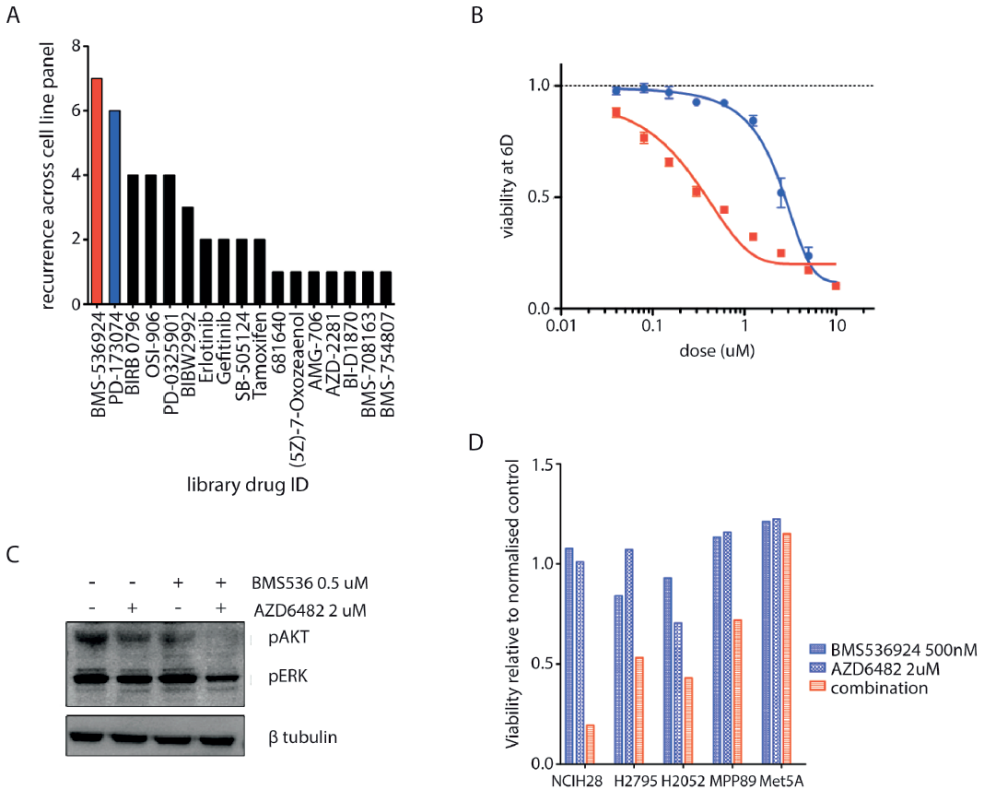

Figure. S8. Combination drug screen of PI3Kinase inhibitor plus drug library in MPM cell lines.

(A) Bar chart showing recurrent synergistic events in a combination screen with PI3K inhibitor AZD6482 plus 95 small molecule inhibitors across 15 MPM cell lines. (B) Validation of synergy between IGF1-R inhibitor BMS-536924 and PI3K inhibitor AZD6482 in NCO-H28 (FGFRi resistant cell line). Dose-response kinetics of BMS-536924 alone (blue) or with fixed dose (2μM) of AZD6482 (red). (C) Immunoblot of NCI-H28 FGFRi resistant cell line treated with a combination of IGF-1R inhibitor BMS-536924 and PI3K inhibitor AZD6482 showing loss of pAKT with combination treatment. (D) Cell Titer Blue quantification of 2 week clonogenic survival assay of 5 MPM cell lines with of IGF-1R inhibitor BMS-536924 alone and in combination with PI3K inhibitor AZD6482.

Table S1. List of compounds used in the chemical inhibitor screen

Identifier	Name	Synonyms	Brand name	Action	Clinical Stage	Putative Target	Targeted process/ pathway
1	Erlotinib	AY-22989,Sirolimus,WY-090217	Tarceva	targeted	clinically approved	EGFR	EGFR signaling
3	Rapamycin		Rapamune	targeted	clinically approved	MTOR	TOR signaling
5	Sunitinib		Sutent	targeted	clinically approved	PDGFRA, PDGFRB, KDR, KIT, FLT3	RTK signaling
6	PHA-665752	zLLL		targeted	experimental	MET	RTK signaling
9	MG-132	BMS-181339-01		targeted	experimental	Proteasome	other
11	Paclitaxel	11-deoxojervine	Taxol	cytotoxic	clinically approved	Microtubules	cytoskeleton
17	Cyclopamine			targeted	experimental	SMO	other
29	AZ628	BAY-43-9006		targeted	experimental	BRAF	ERK MAPK signaling
30	Sorafenib	MK-045,MK-0457,VX-68	Nexavar	targeted	clinically approved	PDGFRA, PDGFRB, KDR, KIT, FLT3	RTK signaling
32	VX-680	STI-571	MK-0457	targeted	in clinical development	AURKA, AURKB, AURKC, FLT3, ABL1, JAK2	mitosis
34	Imatinib	KIN001-017	Gleevec	targeted	clinically approved	ABL, KIT, PDGFR	ABL signaling
35	NVP-TAE684	PF-02341066	TAE684	targeted	experimental	ALK	RTK signaling
37	Crizotinib	Saracatinib,KIN001-045	Xalkori	targeted	in clinical development	MET, ALK	RTK signaling
38	AZD-0530	NSC 83265		targeted	in clinical development	SRC, ABL1	ABL signaling
41	S-Trityl-L-cysteine	Z-L-Norleucine-CHO		targeted	experimental	KIF11	mitosis
45	Z-LLNle-CHO	KIN001-005	na	targeted	experimental	g-secretase	other
51	Dasatinib	KIN001-013 (GNF-2 / 3-(6-(4-(trifluoromethoxy) phenylamino)pyrimidin-4-yl) benzamide)	Sprycel	targeted	clinically approved	ABL, SRC, KIT, PDGFR	ABL signaling

Table S1. Continued

52	GNF-2	KIN001-019		targeted	experimental	ABL [T315I]	ABL signaling
53	CGP-60474	CINK4,KIN001-021		targeted	experimental	CDK1,CDK2,CDK5, CDK7,CDK9	cell cycle
54	CGP-082996	A770041,KIN001-111		targeted	experimental	CDK4	cell cycle
55	A-770041	KIN001-112	A770041	targeted	experimental	SRC family	other
56	WH-4-023	KIN001-123		targeted	experimental	SRC family, ABL	ABL signaling
59	WZ-1-84	KIN001-124		targeted	experimental	BMX	other
60	BI-2536	KIN001-126	NPK33-1-98-1	targeted	in clinical development	PLK1, PLK2, PLK3	mitosis
62	BMS-536924	KIN001-127	BMS-536924	targeted	experimental	IGF1R	IGFR signaling
63	BMS-509744	KIN001-128	BMS-509744	targeted	experimental	ITK	other
64	CMK		Chloromethylketone Rsk inhibitor	targeted	experimental	RSK	ERK MAPK signaling
71	Pyrimethamine		Daraprim	cytotoxic	clinically approved	Dihydrofolate reductase (DHFR)	DNA replication
83	JW-7-52-1	KIN001-139		targeted	experimental	MTOR	TOR signaling
86	A-443654	KIN001-134		targeted	experimental	AKT1, AKT2, AKT3	PI3K signaling
87	GW843682X	MS275	GW843682X (AN-13)	targeted	experimental	PLK1	mitosis
88	MS-275			targeted	in clinical development	HDAC	chromain histone acetylation
89	Parthenolide	KIN001-135		targeted	in clinical development	NFKB1	other
91	KIN001-135			targeted	experimental	IKKE	other
94	TGX221	LDP-341, PS-341		targeted	experimental	PI3Kbeta	PI3K signaling
104	Bortezomib	XMD8-85	Velcade	targeted	clinically approved	Proteasome	other

106	XMD8-85	Seliciclib		targeted	experimental	MAP2K5 (ERK5)	other
110	Roscovitine	3-Phenyl-N-[2,2,2-trichloro-1-[[(8-quinolinylamino) thioxomethyl]amino]ethyl]-2-propenamide		targeted	in clinical development	CDKs	cell cycle
111	Salubrinal	Tykerb, Tyverb		targeted	experimental	GADD34-PP1C	other
119	Lapatinib	KIN001-155	Tykerb, Tyverb	targeted	clinically approved	ERBB2, EGFR	EGFR signaling
127	GSK269962A	Doxil,Rubex		targeted	experimental	ROCK1, ROCK2	cytoskeleton
133	Doxorubicin	VP-16	Adriamycin	cytotoxic	clinically approved	DNA intercalating	DNA replication
134	Etoposide	LY-188011	Etophophos	cytotoxic	clinically approved	TOP2	DNA replication
135	Gemcitabine		Gemzar	cytotoxic	clinically approved	DNA replication	DNA replication
136	Mitomycin C			cytotoxic	clinically approved	DNA crosslinker	DNA replication
140	Vinorelbine		Navelbine	cytotoxic	clinically approved	Microtubules	cytoskeleton
147	NSC-87877	ICI-176334		targeted	experimental	PTPN6 (SHP-1), PTPN11 (SHP-2)	other
150	Bicalutamide	QS11	Casodex	targeted	clinically approved	ANDR (androgen receptor)	other
151	QS11	[2-(6,7-dimethoxyquinazolin-4-yl)-5-(pyridin-2-yl)-2H-1,2,4-triazol-3-amine]		targeted	experimental	ARFGAP	other
152	CP466722	PKC 412		targeted	experimental	ATM	Genome integrity
153	Midostaurin	CT 99021		targeted	in clinical development	KIT	RTK signaling
154	CHIR-99021	KIN001-192		targeted	experimental	GSK3B	WNT signaling
155	AP-24534	KIN001-193	Ponatinib	targeted	in clinical development	ABL	ABL signaling
156	AZD6482	KIN001-204		targeted	in clinical development	PI3Kbeta	PI3K signaling
157	JNK-9L	(KIN001-205)		targeted	experimental	JNK	JNK and p38 signaling
158	PF-562271	KIN001-206		targeted	experimental	FAK	cytoskeleton

Table S1. Continued

159	HG-6-64-1	JQ1		targeted	experimental	BRAFV600E, TAK, MAP4K5	ERK MAPK signaling
163	JQ1	JQ12		targeted	experimental	BRD4	chromatin other
164	JQ12	Dimethyloxalylglcine		targeted	experimental	HDAC	chromain histone acetylation
165	DMOG			targeted	experimental	Prolyl-4-Hydroxylase	other
166	FTI-277	AR-12		targeted	experimental	Farnesyl transferase (FNTA)	other
167	OSU-03012	Shikonin		targeted	experimental	PDPK1 (PDK1)	PI3K signaling
170	Shikonin			not defined	in clinical development	unknown	other
171	AKT inhibitor VIII			targeted	in clinical development	AKT1, AKT2, AKT3	PI3K signaling
172	Embelin	FH535		targeted	in clinical development	XIAP	apoptosis regulation
173	FH535	PAC-1		not defined	experimental	unknown	other
175	PAC-1	IPA-3		targeted	in clinical development	CASP3 agonist	apoptosis regulation
176	IPA-3			targeted	experimental	PAK1, PAK2, PAK3	cytoskeleton
177	GSK-650394			targeted	experimental	SGK3	other
178	BAY 61-3606	5-Fluorouracil		targeted	experimental	SYK	other
179	5-Fluorouracil			cytotoxic	clinically approved	DNA antimetabolite	DNA replication
180	Thapsigargin			targeted	experimental	sarco-endoplasmic reticulum Ca2+-ATPases	other
182	Obatoclax Mesylate		GX15-070	targeted	in clinical development	BCL2, BCL2L1, MCL1	apoptosis regulation
184	BMS-754807	OSI-906		targeted	in clinical development	IGF1R	IGFR signaling

185	OSI-906	LG-100069,LGD-1069		targeted	in clinical development	IGF1R	IGFR signaling
186	Bexarotene		Targretin	targeted	clinically approved	Retinioic acid X family agonist	other
190	Bleomycin	DDE-28		cytotoxic	clinically approved	DNA damage	DNA replication
192	LFM-A13	GW-2580		targeted	experimental	BTK	other
193	GW-2580	VER-52296,NVP-AUY922		targeted	experimental	CSF1R (cFMS)	RTK signaling
194	AUY922	Phenformin		targeted	in clinical development	HSP90	other
196	Phenformin	Bryostatin 1	imidodica_ rbonimidi_c diamide_, N-(2-ph_enylethyl_)-	targeted	experimental	AAPK1 (AMPK) agonist	metabolism
197	Bryostatin 1	GW786034	NSC 339555	targeted	in clinical development	PRKC	other
199	Pazopanib	Dacinostat, NVP-LAQ824	Votrient	targeted	in clinical development	VEGFR, PDGFRA, PDGFRB, KIT	RTK signaling
200	LAQ824	GNF-PF-193		targeted	in clinical development	HDAC	chromain histone acetylation
201	Epothilone B	GSK1904529A	EPO906 (ixabepilone, Patupilone)	cytotoxic	in clinical development	Microtubules	cytoskeleton
202	GSK-1904529A			targeted	experimental	IGF1R	IGFR signaling
203	BMS-345541			targeted	experimental	IKBKB	other
204	Tipifarnib	Avagacestat	Zarnestra,IND58359, R115777	targeted	in clinical development	Farnesyl-transferase (FNTA)	other
205	BMS-708163	INCB-18424		targeted	in clinical development	g-secretase	other
206	Ruxolitinib	AS601245	Jakafi	targeted	clinically approved	JAK1, JAK2, TYK2	other
207	AS601245	Ispinesib Mesylate		targeted	experimental	JNK	JNK and p38 signaling

Table S1. Continued

208	SB-715992			targeted	in clinical development	KIF11	mitosis
211	TL-2-105			targeted	experimental	CRAF	ERK MAPK signaling
219	AT-7519	KIN001-201		targeted	in clinical development	CDK9	cell cycle
221	TAK-715	KIN001-175		targeted	in clinical development	p38a	JNK and p38 signaling
222	BX-912	KIN001-167		targeted	experimental	PDPK1 (PDK1)	PI3K signaling
223	ZSTK474	KIN001-173		targeted	in clinical development	PI3K	PI3K signaling
224	AS605240			targeted	experimental	PI3Kgamma	PI3K signaling
225	Genentech Cpd 10			targeted	experimental	AURKA, AURKB	mitosis
226	GSK1070916			targeted	in clinical development	AURKB	mitosis
228	KIN001-102	Enzastaurin		targeted	experimental	AKT1	PI3K signaling
229	LY317615			targeted	in clinical development	PRKCB (PKCbeta)	other
230	GSK429286A	KIN001-242		targeted	experimental	ROCK2	cytoskeleton
231	FMK			targeted	experimental	RSK	ERK MAPK signaling
235	QL-XII-47			targeted	experimental	BTK, BMX	other
238	CAL-101			targeted	clinically approved	PI3Kdelta	PI3K signaling
245	UNC0638	Cabozantinib		targeted	experimental	G9a(EHMT2), GLP(EHMT1)	chromatin histone methylation
249	XL-184		Cometriq	targeted	clinically approved	VEGFR, MET, RET, KIT, FLT1, FLT3, FLT4, Tie2,AXL	RTK signaling
252	WZ3105			targeted	experimental	CLK2, CNSK1E, FLT3, ULK1	other
253	XMD14-99	Quizartinib, AC-220		targeted	experimental	EPHB3, CAMK1	RTK signaling

254	AC220		targeted	in clinical development	FLT3	RTK signaling
255	CP724714		targeted	in clinical development	ERBB2	EGFR signaling
256	JW-7-24-1		targeted	experimental	LCK	other
257	NPK76-II-72-1		targeted	experimental	PLK3	mitosis
258	STF-62247		not defined	experimental	stimulates autophagy	other
260	NG-25		targeted	experimental	MAP3K7 (TAK1)	other
261	TL-1-85		targeted	experimental	MAP3K7 (TAK1)	other
262	VX-11e		targeted	experimental	ERK	ERK MAPK signaling
263	FR-180204		targeted	experimental	ERK	ERK MAPK signaling
265	Tubastatin A		targeted	experimental	HDAC6	chromain histone acetylation
266	Zibotentan, ZD4054	Sepantronium bromide	targeted	in clinical development	Endothelin A Receptor	other
268	YM155	XI-006	targeted	in clinical development	BIRC5 (Survivin)	apoptosis regulation
269	NSC-207895	4-(Butanoyloxymethyl)phenyl-(2E,4E,6E,8E)-3,7-dimethyl-9-(2,6,6-trimethylcyclohex-1-enyl)nona-2,4,6,8-tetraenoate	targeted	experimental	MDM4	p53 pathway
271	VNLG/124	HDAC-42	targeted	experimental	HDAC, RAR	chromain histone acetylation
272	AR-42		targeted	in clinical development	HDAC	chromain histone acetylation
273	CUDC-101		targeted	in clinical development	HDAC, EGFR	chromain histone acetylation

Table S1. Continued

274	PXD101, Belinostat	GSK525762A,	targeted	clinically approved	HDAC	chromain histone acetylation
275	I-BET 151		targeted	experimental	BRD2, BRD3, BRD4	chromatin other
276	CAY10603		targeted	experimental	HDAC6	chromain histone acetylation
277	ABT-869	Linifanib	targeted	in clinical development	VEGFR and PDGFR family	RTK signaling
279	BIX02189		targeted	experimental	MAP2K5 (MEK5)	other
281	CH5424802		targeted	in clinical development	ALK	RTK signaling
282	EKB-569	Pelitinib	targeted	in clinical development	EGFR	EGFR signaling
283	GSK2126458	EX-8678	targeted	in clinical development	PI3K, MTOR	PI3K signaling
286	KIN001-236		targeted	experimental	TIE2	other
287	KIN001-244		targeted	experimental	PDPK1 (PDK1)	PI3K signaling
288	KIN001-055	WHI-P97, AC1L1GQE	targeted	experimental	JAK3, MNK1	other
290	KIN001-260	Bayer IKKb inhibitor	targeted	experimental	IKK	other
291	KIN001-266		targeted	experimental	MAP3K8 (COT)	other
292	Masitinib	AB1010	targeted	clinically approved	KIT	RTK signaling
293	MP470		targeted	in clinical development	PDGFR	RTK signaling
294	MPS-1-IN-1		targeted	experimental	MPS1	mitosis
295	NVP-BHG712		targeted	experimental	EPHB4	RTK signaling
298	OSI-930		targeted	in clinical development	KIT, VEGFR, PDGFR	RTK signaling

299	OSI-027	activebiochem A-1065	targeted	in clinical development	MTORC1/2	TOR signaling
300	CX-5461		targeted	experimental	RNA Pol I	other
301	PHA-793887		targeted	experimental	CDK-pan	cell cycle
302	PI-103		targeted	experimental	PI3Ka, PRKDC (DNAPK)	PI3K signaling
303	PIK-93		targeted	experimental	PI4K, PI3K	PI3K signaling
304	SB52334		targeted	experimental	ALK5	RTK signaling
305	TPCA-1		targeted	experimental	IKK	other
306	TG101348		targeted	in clinical development	JAK2	other
308	XL-880	GSK1363089, foretinib	targeted	in clinical development	MET	RTK signaling
309	Y-39983		targeted	experimental	ROCK	cytoskeleton
310	YM201636		targeted	experimental	FYV1	other
312	AV-951	Tivozanib	targeted	in clinical development	VEGFR	RTK signaling
326	GSK690693		targeted	experimental	AKT	PI3K signaling
328	SNX-2112		targeted	experimental	HSP90	other
329	QL-XI-92		targeted	experimental	DDR1	RTK signaling
330	XMD13-2		targeted	experimental	RIPK	other
331	QL-X-138		targeted	experimental	MNK2, PRKDC (DNAPK), MTOR, BTK, JAK3	other
332	XMD15-27		targeted	experimental	CAMK2B, CLK2, DYRK1A, MAST1, STK39	other
333	T0901317		targeted	experimental	LXR	other
341	EX-527		targeted	experimental	SIRT1	other
344	THZ-2-49		targeted	experimental	CDK9	cell cycle

Table S1. Continued

345	KIN001-270			targeted	experimental	CDK9	cell cycle
346	THZ-2-102-1			targeted	experimental	CDK7	cell cycle
1001	AICAR	N1-(b-D-Ribofuranosyl)-5-aminoimidazole-4-carboxamide	AICAR	targeted	in clinical development	AAPK1 (AMPK) agonist	metabolism
1003	Camptothecin	7-Ethyl-10-Hydroxy-Camptothecin,SN-38	SN-38	cytotoxic	clinically approved	TOP1	DNA replication
1004	Vinblastine	Vinblastine sulphate	Vinblastine	cytotoxic	clinically approved	Microtubules	cytoskeleton
1005	Cisplatin	cis-Diammineplatinum(II) dichloride	Cisplatin	cytotoxic	clinically approved	DNA crosslinker	DNA replication
1006	Cytarabine	Ara-Cytidine,Arabinosyl Cytosine,U-19920	Cytarabine (AraC)	cytotoxic	clinically approved	DNA synthesis	DNA replication
1007	Docetaxel	RP-56976	Taxotere	cytotoxic	clinically approved	Microtubules	cytoskeleton
1008	Methotrexate		Methotrexate	cytotoxic	clinically approved	Dihydrofolate reductase (DHFR)	DNA replication
1009	ATRA	Tretinoin	Vesanoid	targeted	clinically approved	Retinoic acid and retinoid X receptor agonist	other
1010	Gefitinib	ZD-1839	Iressa	targeted	clinically approved	EGFR	EGFR signaling
1011	ABT-263			targeted	in clinical development	BCL2, BCL2L1, BCL2L2	apoptosis regulation
1012	Vorinostat	SAHA	Zolinza	targeted	clinically approved	HDAC inhibitor Class I, IIa, IIb, IV	chromain histone acetylation
1013	Nilotinib		Tasigna	targeted	clinically approved	ABL	ABL signaling
1014	RDEA119	RDEA119		targeted	in clinical development	MAP2K1 (MEK1), MAP2K2 (MEK2)	ERK MAPK signaling
1015	CI-1040	PD-18435,PD-184352		targeted	in clinical development	MAP2K1 (MEK1), MAP2K2 (MEK2)	ERK MAPK signaling
1016	Temsirolimus	CCI-779	Torisel	targeted	clinically approved	MTOR	TOR signaling
1017	Olaparib	KU-0059436, AZD-2281	Lynparza	targeted	in clinical development	PARP1, PARP2	Genome integrity

1018	ABT-888	ABT-888		targeted	in clinical development	PARP1, PARP2	Genome integrity
1019	Bosutinib	SKI-606	Bosulif	targeted	clinically approved	SRC, ABL, TEC	ABL signaling
1020	Lenalidomide		Revlimid	targeted	clinically approved	TNFA	other
1021	Axitinib	AG-013736	Axitinib	targeted	in clinical development	PDGFR, KIT, VEGFR	RTK signaling
1022	AZD7762	AZD 7762		targeted	in clinical development	CHEK1, CHEK2	Genome integrity
1023	GW 441756			targeted	experimental	NTRK1	RTK signaling
1024	CEP-701	CEP-701	Lestaurtinib	targeted	in clinical development	FLT3, JAK2, NTRK1, RET	RTK signaling
1025	SB 216763	SB 216763		targeted	experimental	GSK3A, GSK3B	WNT signaling
1026	17-AAG	17-AAG	Telatinib	targeted	in clinical development	HSP90	other
1028	VX-702			targeted	in clinical development	p38	JNK and p38 signaling
1029	AMG-706	AMG-706	Motesanib Diphosphate	targeted	in clinical development	VEGFR, RET, c-KIT, PDGFR	RTK signaling
1030	KU-55933			targeted	experimental	ATM	Genome integrity
1031	Elesclomol			targeted	in clinical development	HSP70	other
1032	Afatinib	Tovok, BIBW2992	Gilotrif	targeted	clinically approved	ERBB2, EGFR	EGFR signaling
1033	Vismodegib	GDC-0449	Erivedge	targeted	in clinical development	SMO	other
1036	PLX4720	Vemurafenib (derivative)	Zelboraf (derivative)	targeted	clinically approved	BRAF	ERK MAPK signaling
1037	BX-795	BX 795		targeted	in clinical development	TBK1, PDPK1, IKK, AURKB, AURKC	other
1038	NU-7441	NU-7432,KU-57788		targeted	experimental	PRKDC (DNAPK)	Genome integrity

Table S1. Continued

1039	SL 0101-1			targeted	experimental	RSK, AURKB, PIM3	ERK MAPK signaling
1042	BIRB 0796		Doramapimod	targeted	experimental	p38, JNK2	JNK and p38 signaling
1043	JNK Inhibitor VIII	JNK Inhibitor VIII		targeted	experimental	JNK	JNK and p38 signaling
1046	681640,00	681640,00		targeted	experimental	WEE1, CHEK1	cell cycle
1047	Nutlin-3a	Nutlin-3a (-) enantiomer		targeted	in clinical development	MDM2	p53 pathway
1049	PD-173074	PD-173074		targeted	experimental	FGFR1, FGFR3	RTK signaling
1050	ZM-447439	ZM447439		targeted	experimental	AURKB	mitosis
1052	RO-3306			targeted	experimental	CDK1	cell cycle
1053	MK-2206			targeted	in clinical development	AKT1, AKT2	PI3K signaling
1054	PD-0332991	PD-0332991		targeted	in clinical development	CDK4, CDK6	cell cycle
1057	NVP-BEZ235	BEZ235		targeted	in clinical development	PI3K (Class 1) and MTORC1/2	PI3K signaling
1058	GDC0941			targeted	in clinical development	PI3K (class 1)	PI3K signaling
1059	AZD8055	AZD8055	pp242	targeted	in clinical development	MTORC1/2	TOR signaling
1060	PD-0325901	PD-0325901		targeted	in clinical development	MAP2K1 (MEK1), MAP2K2 (MEK2)	ERK MAPK signaling
1061	SB590885			targeted	experimental	BRAF	ERK MAPK signaling
1062	AZD6244			targeted	in clinical development	MAP2K1 (MEK1), MAP2K2 (MEK2)	ERK MAPK signaling
1066	AZD6482	WO2009093972		targeted	in clinical development	PI3Kbeta	PI3K signaling
1067	CCT007093			targeted	experimental	PPM1D	other

1069	EHT 1864			targeted	experimental	Rac GTPases	cytoskeleton
1072	BMS-708163	Avagacestat		targeted	in clinical development	g-secretase	other
1091	BMS-536924	BMS-536924		targeted	experimental	IGF1R	IGFR signaling
1114	Cetuximab	Cetuximab	Erbitux	targeted	clinically approved	EGFR	EGFR signaling
1129	PF-4708671			targeted	experimental	RPS6KB1 (p70S6KA)	TOR signaling
1133	JNJ-26854165		Serdemetan	targeted	in clinical development	MDM2	p53 pathway
1142	HG-5-113-01			targeted	in clinical development	LOK, LTK, TRCB, ABL(T315I)	ABL signaling
1143	HG-5-88-01			targeted	experimental	EGFR, ADCK4	EGFR signaling
1149	TW 37			targeted	experimental	BCL2, BCL2L1	apoptosis regulation
1158	XMD11-85h			targeted	experimental	BRSK2, FLT4, MARK4, PRKCD, RET, SPRK1	other
1161	ZG-10			targeted	experimental	IRAK1	other
1164	XMD8-92			targeted	experimental	MAP2K5 (ERK5)	other
1166	QL-VIII-58			targeted	experimental	MTOR, ATR	TOR signaling
1170	CCT018159			targeted	experimental	HSP90	other
1175	AG-014699	PF-01367338		targeted	experimental	PARP1, PARP2	Genome integrity
1192	GSK269962A	KIN001-155		targeted	experimental	ROCK1, ROCK2	cytoskeleton
1194	SB-505124	2-(5-Benzo[1,3]dioxol-5-yl-2-tert-butyl-3H-imidazol-4-yl)-6-methylpyridine hydrochloride hydrate		targeted	experimental	TGFR1 (ALK5)	other
1199	Tamoxifen			targeted	clinically approved	ER	other
1203	QL-XII-61			targeted	experimental	BTK	other
1218	JQ1			targeted	experimental	BRD2, BRD3, BRD4	chromatin other

Table S1. Continued

1219	PFI-1			targeted	experimental	BRD2, BRD3, BRD4	chromatin other
1230	IOX2			targeted	experimental	EGLN1	other
1236	UNC0638			targeted	experimental	G9a(EHMT2), GLP(EHMT1)	chromatin histone methylation
1239	YK 4-279			targeted	experimental	RNA helicase A	other
1241	CHIR-99021	CT 99021		targeted	experimental	GSK3B	WNT signaling
1242	(5Z)-7-Oxozeaenol			targeted	experimental	MAP3K7 (TAK1)	other
1243	piperlongumine			not defined	experimental	Increases ROS levels	other
1248	FK866	APO866		targeted	experimental	NAMPT	metabolism
1259	BMN-673			targeted	experimental	PARP1	Genome integrity
1261	rTRAIL			targeted	experimental	TR10A (DR4), TR10B (DR5)	apoptosis regulation
1262	UNC1215			targeted	experimental	LMBL3	other
1264	SGC0946			targeted	experimental	Q8TEK3 (DOT1L)	chromatin histone methylation
1268	XAV 939	NVP-XAV 939		targeted	experimental	TNKS1 (tankyrase-1)	WNT signaling
1371	PLX4720 (rescreen)	Vemurafenib (derivative)	Zelboraf	targeted	experimental	BRAF	ERK MAPK signaling
1372	Trametinib	GSK1120212	Mekinist	targeted	clinically approved	MAP2K1 (MEK1), MAP2K2 (MEK2)	ERK MAPK signaling
1373	Dabrafenib	GSK2118436	Tafinlar	targeted	clinically approved	BRAF	ERK MAPK signaling
1375	Temozolomide	Temodar		cytotoxic	clinically approved	DNA akylating agent	DNA replication
1377	Afatinib (rescreen)	Tovok, BIBW2992	Gilotrif	targeted	clinically approved	ERBB2, EGFR	EGFR signaling

1378	Bleomycin (50 uM)			cytotoxic	clinically approved	DNA damage	DNA replication
1494	SN-38	7-ETHYL-10-HYDROXY-CAMPTOTHECIN		cytotoxic	experimental	TOP1	DNA replication
1495	Olaparib	Olaparib		targeted	clinically approved	PARP1, PARP2	Genome integrity
1498	AZD6244			targeted	in clinical development	MAP2K1 (MEK1), MAP2K2 (MEK2)	ERK MAPK signaling
1502	Bicalutamide	ICI-176334	Casodex	targeted	clinically approved	ANDR (androgen receptor)	other
1526	RDEA119 (rescreen)			targeted	experimental	MAP2K1 (MEK1), MAP2K2 (MEK2)	ERK MAPK signaling
1527	GDC0941 (rescreen)			targeted	in clinical development	PI3K	PI3K signaling
1529	MLN4924			targeted	in clinical development	NEDD8-activating enzyme	other

Table S2. SPIA pathway analysis performed highlighting significantly upregulated/downregulated pathways between BAP1 mutant and BAP1 wild type lines.

Name	ID	pSize	NDE	pNDE	tA	pPERT	pG
Complement and coagulation cascades	4610	67	1	0,239757502	16,87317213	0,004	0,007623894
Gap junction	4540	85	2	0,047099152	6,9486621	0,03	0,010684996
MAPK signaling pathway	4010	260	5	0,004188945	1,872639843	0,393	0,01219752
Glioma	5214	62	2	0,026481172	5,769688959	0,125	0,022213608
Prostate cancer	5215	88	2	0,05011322	5,902911432	0,068	0,022769284
Melanoma	5218	71	2	0,033994969	7,652553716	0,169	0,035386672
Protein processing in endoplasmic reticulum	4141	161	1	0,483342609	2,760670737	0,025	0,06544349
Focal adhesion	4510	198	2	0,193196516	5,353545369	0,141	0,125390148
HTLV-I infection	5166	259	2	0,284858199	2,25223501	0,151	0,178344625
Cytokine-cytokine receptor interaction	4060	248	2	0,268225286	1,4263907	0,163	0,180563656
Bladder cancer	5219	40	1	0,150861921	0,28656377	0,294	0,182539356
Regulation of actin cytoskeleton	4810	212	3	0,055678487	-1,134243636	0,798	0,182782389
Neurotrophin signaling pathway	4722	117	2	0,082459008	-2,062560979	0,586	0,194728203
Pancreatic cancer	5212	69	1	0,24596437	1,146255078	0,256	0,237079519
Endometrial cancer	5213	52	1	0,191570826	0,764170052	0,339	0,242511753
Pathways in cancer	5200	321	2	0,377272508	3,238496438	0,188	0,258607838
Non-small cell lung cancer	5223	54	1	0,198165792	0,818753627	0,381	0,270566523
ErbB signaling pathway	4012	86	1	0,29674309	1,152623162	0,262	0,276335005
Oocyte meiosis	4114	106	1	0,352175452	-2,13630758	0,242	0,295091787
Cell cycle	4110	122	1	0,393397279	1,022863241	0,41	0,45557714
Apoptosis	4210	87	1	0,299622651	-1,11934781	0,547	0,46030136
Vasopressin-regulated water reabsorption	4962	44	1	0,164651424	0	1	0,461670182
Hepatitis C	5160	129	1	0,410607473	0,28656377	0,452	0,498171235
Mineral absorption	4978	51	1	0,188253298	0	1	0,502630073
Tuberculosis	5152	171	1	0,504199822	0,780592299	0,377	0,505677304
Amyotrophic lateral sclerosis (ALS)	5014	52	1	0,191570826	0	1	0,508141173
Insulin signaling pathway	4910	134	1	0,422604562	1,11934781	0,46	0,512792474
Axon guidance	4360	127	1	0,405740054	2,22E-16	0,535	0,548653527
Adipocytokine signaling pathway	4920	68	1	0,242867213	0	1	0,586582712
PPAR signaling pathway	3320	70	1	0,249049025	0	1	0,595253447
Phosphatidylinositol signaling system	4070	77	1	0,270295671	0	1	0,623906966
Lysosome	4142	119	1	0,385870539	0	1	0,753317055
Measles	5162	127	1	0,405740054	0	1	0,771734861
Alcoholism	5034	129	1	0,410607473	0	1	0,776096401
RNA transport	3013	146	1	0,450423166	0	1	0,809666166
Transcriptional misregulation in cancer	5202	156	1	0,47259166	0	1	0,826810244
Herpes simplex infection	5168	173	1	0,508270435	0	1	0,852238193
Calcium signaling pathway	4020	178	1	0,51830324	0	1	0,858929435

pGFdr	pGFWER	Status	KEGGLINK
0,154501919	0,289707958	Activated	http://www.genome.jp/dbget-bin/show_pathway?hsa04610+7035
0,154501919	0,406029842	Activated	http://www.genome.jp/dbget-bin/show_pathway?hsa04540+1950+5154
0,154501919	0,463505756	Activated	http://www.genome.jp/dbget-bin/show_pathway?hsa04010+4915+8912+5154+1950+51347
0,173046556	0,844117116	Activated	http://www.genome.jp/dbget-bin/show_pathway?hsa05214+1950+5154
0,173046556	0,865232778	Activated	http://www.genome.jp/dbget-bin/show_pathway?hsa05215+1950+5154
0,224115586	1	Activated	http://www.genome.jp/dbget-bin/show_pathway?hsa05218+1950+5154
0,355264658	1	Activated	http://www.genome.jp/dbget-bin/show_pathway?hsa04141+258010
0,569205517	1	Activated	http://www.genome.jp/dbget-bin/show_pathway?hsa04510+1950+5154
0,569205517	1	Activated	http://www.genome.jp/dbget-bin/show_pathway?hsa05166+9184+5154
0,569205517	1	Activated	http://www.genome.jp/dbget-bin/show_pathway?hsa04060+1950+5154
0,569205517	1	Activated	http://www.genome.jp/dbget-bin/show_pathway?hsa05219+1950
0,569205517	1	Inhibited	http://www.genome.jp/dbget-bin/show_pathway?hsa04810+10152+1950+5154
0,569205517	1	Inhibited	http://www.genome.jp/dbget-bin/show_pathway?hsa04722+4915+397
0,5833739	1	Activated	http://www.genome.jp/dbget-bin/show_pathway?hsa05212+1950
0,5833739	1	Activated	http://www.genome.jp/dbget-bin/show_pathway?hsa05213+1950
0,5833739	1	Activated	http://www.genome.jp/dbget-bin/show_pathway?hsa05200+1950+5154
0,5833739	1	Activated	http://www.genome.jp/dbget-bin/show_pathway?hsa05223+1950
0,5833739	1	Activated	http://www.genome.jp/dbget-bin/show_pathway?hsa04012+1950
0,590183573	1	Inhibited	http://www.genome.jp/dbget-bin/show_pathway?hsa04114+9748
0,721707926	1	Activated	http://www.genome.jp/dbget-bin/show_pathway?hsa04110+9184
0,721707926	1	Inhibited	http://www.genome.jp/dbget-bin/show_pathway?hsa04210+5575
0,721707926	1	Inhibited	http://www.genome.jp/dbget-bin/show_pathway?hsa04962+397
0,721707926	1	Activated	http://www.genome.jp/dbget-bin/show_pathway?hsa05160+1950
0,721707926	1	Inhibited	http://www.genome.jp/dbget-bin/show_pathway?hsa04978+26872
0,721707926	1	Activated	http://www.genome.jp/dbget-bin/show_pathway?hsa05152+9902
0,721707926	1	Inhibited	http://www.genome.jp/dbget-bin/show_pathway?hsa05014+4747
0,721707926	1	Activated	http://www.genome.jp/dbget-bin/show_pathway?hsa04910+5575
0,744601216	1	Activated	http://www.genome.jp/dbget-bin/show_pathway?hsa04360+64221
0,7539877	1	Inhibited	http://www.genome.jp/dbget-bin/show_pathway?hsa04920+2182
0,7539877	1	Inhibited	http://www.genome.jp/dbget-bin/show_pathway?hsa03320+2182
0,764789184	1	Inhibited	http://www.genome.jp/dbget-bin/show_pathway?hsa04070+3628
0,858929435	1	Inhibited	http://www.genome.jp/dbget-bin/show_pathway?hsa04142+2581
0,858929435	1	Inhibited	http://www.genome.jp/dbget-bin/show_pathway?hsa05162+9367
0,858929435	1	Inhibited	http://www.genome.jp/dbget-bin/show_pathway?hsa05034+4915
0,858929435	1	Inhibited	http://www.genome.jp/dbget-bin/show_pathway?hsa03013+9939
0,858929435	1	Inhibited	http://www.genome.jp/dbget-bin/show_pathway?hsa05202+5154
0,858929435	1	Inhibited	http://www.genome.jp/dbget-bin/show_pathway?hsa05168+6431
0,858929435	1	Inhibited	http://www.genome.jp/dbget-bin/show_pathway?hsa04020+8912

Table S3. GEO data analysis of 40 BAP1 wild type versus 11 BAP1 mutant mesothelioma tumors showing fold change in mRNA expression.

ID	adj.P.Val	P.Value	t	B	logFC	Gene.symbol	Gene.title
206987_x_at	**0,0467**	8,40E-06	-4,9297914	2,074	-1,55210916	**FGF18**	fibroblast growth factor 18
211029_x_at	**0,0331**	3,23E-06	-5,200056	2,71569	-1,46628317	**FGF18**	fibroblast growth factor 18
211485_s_at	**0,0173**	7,78E-07	-5,5953934	3,66039	-1,32935104	**FGF18**	fibroblast growth factor 18
203638_s_at	0,8387	9,17E-02	-1,7172855	-4,20483	-0,58459186	**FGFR2**	fibroblast growth factor receptor 2
208228_s_at	0,8261	7,39E-02	-1,822761	-4,07017	-0,57807812	**FGFR2**	fibroblast growth factor receptor 2
205110_s_at	0,7406	2,47E-02	-2,3120189	-3,35944	-0,57359639	**FGF13**	fibroblast growth factor 13
203639_s_at	0,8385	8,69E-02	-1,7439568	-4,17143	-0,42430659	**FGFR2**	fibroblast growth factor receptor 2
204379_s_at	0,7207	1,73E-02	-2,4574403	-3,12282	-0,30363692	**FGFR3**	fibroblast growth factor receptor 3
214284_s_at	0,7144	8,97E-03	-2,7123752	-2,68264	-0,2416635	**FGF18**	fibroblast growth factor 18
215404_x_at	0,7195	1,54E-02	2,5044305	-3,04406	0,32050106	**FGFR1**	fibroblast growth factor receptor 1